



Large uncertainties in future biome changes in Africa call for flexible climate adaptation strategies

Carola Martens^{1,2} | Thomas Hickler^{1,2} | Claire Davis-Reddy³ |
Francois Engelbrecht⁴ | Steven I. Higgins⁵ | Graham P. von Maltitz^{6,7} |
Guy F. Midgley⁷ | Mirjam Pfeiffer² | Simon Scheiter²

¹Institute of Physical Geography, Goethe University Frankfurt am Main, Frankfurt am Main, Germany

²Senckenberg Biodiversity and Climate Research Centre (SBIK-F), Frankfurt am Main, Germany

³uLwazi Node, South African Environmental Observation Network (SAEON), Cape Town, South Africa

⁴Global Change Institute, University of the Witwatersrand, Johannesburg, South Africa

⁵Plant Ecology, University of Bayreuth, Bayreuth, Germany

⁶Council for Scientific and Industrial Research (CSIR), Pretoria, South Africa

⁷Global Change Biology Group, Stellenbosch University, Stellenbosch, South Africa

Correspondence

Carola Martens, Institute of Physical Geography, Goethe University Frankfurt am Main, Altenhöferallee 1, 60438 Frankfurt am Main, Germany.
Email: martens.carola@yahoo.de

Funding information

Bundesministerium für Bildung und Forschung, Grant/Award Number: 01LL1801B and 01LL1802B; Alexander von Humboldt-Stiftung; Deutsche Forschungsgemeinschaft, Grant/Award Number: SCHE 1719/2-1; National Research Foundation, Grant/Award Number: 11859

Abstract

Anthropogenic climate change is expected to impact ecosystem structure, biodiversity and ecosystem services in Africa profoundly. We used the adaptive Dynamic Global Vegetation Model (aDGVM), which was originally developed and tested for Africa, to quantify sources of uncertainties in simulated African potential natural vegetation towards the end of the 21st century. We forced the aDGVM with regionally downscaled high-resolution climate scenarios based on an ensemble of six general circulation models (GCMs) under two representative concentration pathways (RCPs 4.5 and 8.5). Our study assessed the direct effects of climate change and elevated CO₂ on vegetation change and its plant-physiological drivers. Total increase in carbon in aboveground biomass in Africa until the end of the century was between 18% to 43% (RCP4.5) and 37% to 61% (RCP8.5) and was associated with woody encroachment into grasslands and increased woody cover in savannas. When direct effects of CO₂ on plants were omitted, woody encroachment was muted and carbon in aboveground vegetation changed between -8 to 11% (RCP 4.5) and -22 to -6% (RCP8.5). Simulated biome changes lacked consistent large-scale geographical patterns of change across scenarios. In Ethiopia and the Sahara/Sahel transition zone, the biome changes forecast by the aDGVM were consistent across GCMs and RCPs. Direct effects from elevated CO₂ were associated with substantial increases in water use efficiency, primarily driven by photosynthesis enhancement, which may relieve soil moisture limitations to plant productivity. At the ecosystem level, interactions between fire and woody plant demography further promoted woody encroachment. We conclude that substantial future biome changes due to climate and CO₂ changes are likely across Africa. Because of the large uncertainties in future projections, adaptation strategies must be highly flexible. Focused research on CO₂ effects, and improved model representations of these effects will be necessary to reduce these uncertainties.

KEYWORDS

aDGVM, biome shifts and transitions, carbon stocks, climate change, CO₂ fertilization, ensemble simulations, uncertainties, water use efficiency

This is an open access article under the terms of the Creative Commons Attribution License, which permits use, distribution and reproduction in any medium, provided the original work is properly cited.

© 2020 The Authors. *Global Change Biology* published by John Wiley & Sons Ltd

1 | INTRODUCTION

Climate change is expected to drive changes in ecosystem structure and functioning as well as geographical shifts of ecosystems and biomes (Engelbrecht & Engelbrecht, 2016; Hoegh-Guldberg et al., 2018; Niang et al., 2014). Such ecosystem changes will impact the potential for future land uses and the livelihoods of people in Africa, where agriculture accounted for ~50% of employment in 2019 (ILO, 2019). The critical ecosystem services provided vary for different biomes (Chapin et al., 2011, p. 428), such as carbon sequestration (forests), and pasture for grazing (grasslands and savannas, Naidoo et al., 2008). Biome changes and shifts therefore impact ecosystem services (Gonzalez et al., 2010). Furthermore, many animal species are strongly associated with certain biome types (Jetz & Fine, 2012), which together with vegetation changes implies large potential impacts on prevailing biodiversity.

Biome shifts attributed to climate change have already been observed in Africa (Niang et al., 2014), but do not show a consistent pattern. For instance, declines in tree density and changes in species composition have led to a southward shift of the savanna vegetation zone in West Africa (Gonzalez et al., 2012) into previously more humid areas. At the same time, increased woody cover in savannas has been reported at many sites across Africa, including West Africa. Increasing atmospheric CO₂ concentrations ([CO₂]), changes in land management and altered rainfall patterns were identified as likely drivers of this woody vegetation increase (Stevens et al., 2017).

With the widespread mixture of grasses with C₄ photosynthesis and woody plants with C₃ photosynthesis across African savannas, plant-physiological effects of increasing [CO₂] might change the competitive balance between grasses and trees and thus play a key role for future ecosystem changes (Bond & Midgley, 2000; Midgley & Bond, 2015; Osborne et al., 2018). Furthermore, changes in plant growth interact with changes in fire regimes, and direct enhancement of tree sapling growth rates under elevated [CO₂] (eCO₂) increases the likelihood that young tree individuals escape the 'firetrap'. This might lead to a positive feedback, where an initial increase in woody vegetation suppresses grasses, thereby reduces fire activity, which in turn benefits woody plants (Bond & Midgley, 2012; Midgley & Bond, 2015).

However, the magnitude of eCO₂ effects, both directly on plant growth through CO₂ fertilization of photosynthetic efficiency (Long et al., 2004) and indirectly on ecosystem hydrology (through a reduction of stomatal conductance, g_s ; Ainsworth & Rogers, 2007; Medlyn et al., 2001), is still debated (Körner, 2015; Medlyn et al., 2015; Zaehle et al., 2014). Free-Air carbon dioxide enrichment (FACE) experiments suggest that an increase in carbon assimilation in C₃ plants does not necessarily scale to increased plant growth (e.g. Körner et al., 2005; Medlyn et al., 2015), particularly when limited by nutrient availability (e.g. Jiang, Caldararu, et al., 2020; Jiang, Medlyn, et al., 2020; Norby et al., 2010). For ecosystem hydrology and water use efficiency (WUE), eCO₂ effects translate into a balance of decreased transpiration and water demand due to reduced g_s (De Kauwe et al., 2013) and increased water demand following increased net primary production (NPP; Warren et al., 2011).

Dynamic Global Vegetation Models (DGVMs) are a widely used tool to project future ecosystem changes and to attribute ongoing changes to different drivers and mechanisms (Prentice et al., 2007). DGVMs simulate ecophysiological processes, such as photosynthesis and plant growth, vegetation dynamics and structure, geographical distribution of plant biomes and biogeochemical cycles (e.g. water and carbon), in particular in response to climate change (e.g. Prentice et al., 2007; Sitch et al., 2008). However, the effects of eCO₂ on plants and interactions with nutrient limitations in DGVMs are still uncertain (Hickler et al., 2015; Medlyn et al., 2015). If key plant demographic processes such as mortality, recruitment of tree saplings and fire impacts on plant individuals are implemented in DGVMs (Fisher et al., 2018), they can capture complex dynamics in savanna ecosystems.

In this study, we simulated the impacts of climate change and eCO₂ on carbon stocks, WUE and biome distribution of potential natural vegetation (PNV) in Africa using the adaptive Dynamic Global Vegetation Model (aDGVM; Scheiter & Higgins, 2009). The aDGVM was originally developed for Africa and its savannas (Scheiter & Higgins, 2009) and has been applied and tested in several Africa-focused case studies (e.g. Scheiter et al., 2018; Scheiter & Savadogo, 2016). It simulates woody plant demography for individual trees and this allows fire impacts to be conditioned on individual tree size. Advancing on earlier studies with the aDGVM, we used an ensemble of regional climate model (RCM) data based on six downscaled general circulation models (GCMs; Archer et al., 2018; Davis-Reddy et al., 2017; Engelbrecht et al., 2015) and two Representative Concentration Pathway (RCP) scenarios (RCPs 4.5 and 8.5, Stocker et al., 2013). This is the first time that this ensemble of downscaled GCM data has been used as a climate driver for a DGVM covering Africa. We ran the aDGVM with and without eCO₂ effects enabled to assess uncertainty related to plant-physiological CO₂ effects and to identify important drivers of vegetation change. Our study quantifies how uncertainty in projections caused by CO₂, in particular concerning CO₂ effects on WUE and biomass, interacts with uncertainty due to the choice of GCM and RCP.

2 | MATERIALS AND METHODS

2.1 | The aDGVM

For this study, we used the well-tested aDGVM, a regionally adapted DGVM (e.g. Scheiter & Higgins, 2009; Scheiter et al., 2015; Scheiter & Savadogo, 2016). The aDGVM was developed for tropical and subtropical grass-tree ecosystems (for details, see Scheiter & Higgins, 2009; Scheiter et al., 2012). It incorporates ecophysiological processes that are commonly implemented in DGVMs (Prentice et al., 2007). State variables such as photosynthetic rates, biomass or height are simulated for individual plants depending on environmental conditions. For each plant the aDGVM dynamically simulates leaf phenology and flexibly determines carbon allocation to plant biomass compartments (roots, stem or leaf biomass). aDGVM prioritizes carbon allocation to compartments that are most limiting

for plant growth based on the constraining factors water, light or photosynthesis. Physiological processes, such as photosynthesis, g_s and transpiration, are simulated for each individual plant based on environmental and plant individual state variables such as light availability. Stomatal conductance is represented by the model from Ball et al. (1987) and is directly proportional to relative humidity, and the ratio of photosynthesis and $[CO_2]$ at the leaf surface (Medlyn et al., 2001).

The aDGVM simulates 1-ha plots that are assumed to be representative for the simulated grid cell. Grasses with C_3 and C_4 photosynthesis are each implemented as two types of super-individuals that represent grasses growing beneath tree canopies and in tree canopy gaps. The aDGVM distinguishes savanna and forest trees (Scheiter et al., 2012) as two distinct tree types that differ in their fire and shade tolerance (Bond & Midgley, 2001; Ratnam et al., 2011). In the model, savanna trees are shade intolerant and more fire resistant as adult trees (>2 m). Modelled forest trees are shade tolerant but fire sensitive in all age classes. Each tree individual competes for light with neighbouring plants and for water with all plants simulated per 1-ha plot.

Fire in the aDGVM is determined by fuel load and fuel moisture, both dependent on biomass growth and thus indirectly influenced by climate, and wind speed following Higgins et al. (2008). Ignitions are simulated as random events decoupled from climatic or regional factors. Fire disturbance is therefore one of the factors causing some stochasticity in the model results. Whether fire spreads after a stochastic ignition event depends on fire intensity and a previously determined likelihood that a fire will spread (Scheiter & Higgins, 2009).

In contrast to many other DGVMs, simulating individual trees in aDGVM allows accounting for fire effects on individual plants and vegetation structure as a function of individual plant height (Scheiter & Higgins, 2009). Height influences if trees survive grass fires because only tall enough trees can escape the flame or topkill zone of a fire (Higgins et al., 2000). In addition, in contrast to forest trees, grasses and savanna trees in aDGVM are able to resprout after fire damage (Bond & Midgley, 2001). Population composition evolves dynamically in the model as a result of interactions of, for example, fire and $[CO_2]$. Random events in demography subroutines for tree populations add to the stochasticity in model results.

2.2 | Regional climate model simulations

Climate input data consisted of an ensemble of six downscaled GCM projections under two mitigation scenarios generated with the variable-resolution conformal-cubic atmospheric model (CCAM; McGregor, 2005). The simulations were performed at the Council for Scientific and Industrial Research in South Africa (Archer et al., 2018; Davis-Reddy et al., 2017; Engelbrecht et al., 2015). The GCM projections formed part of the Coupled Model Intercomparison Project Phase 5 (CMIP5; Table S1; Stocker et al., 2013). The downscaling procedure involved CCAM being integrated globally at a quasi-uniform

resolution of about 50 km in the horizontal, forced at its lower boundary by sea-ice concentrations and bias-corrected sea-surface temperatures from the host GCMs (Engelbrecht et al., 2015). The CCAM simulations were performed for the period 1961–2099 and for the low mitigation scenario RCP8.5 and modest-high mitigation scenario RCP4.5.

The downscaled climate data sets were bias-corrected to the monthly climatologies of temperature and rainfall from CRU TS3.1 data for the period 1961–1990 (Engelbrecht & Engelbrecht, 2016; Engelbrecht et al., 2015). Previously, the CCAM downscalings have been shown to realistically represent present-day climate over southern Africa (e.g. Engelbrecht et al., 2009, 2013, 2015).

CCAM output is available on a latitude–longitude grid of 0.5° resolution and at a daily time step. We used daily precipitation, daily minimum and maximum temperature, daily wind speed and daily relative humidity from the CCAM data set to force aDGVM (see Figure S1 for mean annual precipitation (MAP) and temperature maps). As projected radiation data were not available, we derived present-day radiation from sunshine percentage (Allen et al., 1998) from New et al. (2002). Thus, our vegetation simulations are based on an ensemble of climate data providing a range of GCM-projected climate change under two emission scenarios at high spatial and temporal resolution.

2.3 | Simulation design

We simulated vegetation dynamics in Africa from 1971 to 2099 at 0.5° resolution by forcing the aDGVM with the climate ensemble described above and soil data from the Global Soil Data Task Group (2000). A model spin-up of 210 years was simulated to allow vegetation to reach equilibrium with environmental forcing. To that end, we used a random series of climate data from the period 1971–1979. In our experimental setup, we combined changes in climatic conditions with increases in $[CO_2]$ (eCO_2) for two greenhouse gas emission scenarios, RCPs 4.5 and 8.5. To estimate the extent of the eCO_2 effect and its uncertainties, we repeated the same simulations with climate conditions following the two RCP scenarios, but with $[CO_2]$ rising only to 400 ppm and then keeping $[CO_2]$ fixed (fCO_2).

Stochastic effects within DGVMs can be factored in when conducting replicate runs for each ensemble member. Due to high computing times for continental-scale high-resolution simulations, for each GCM only one simulation was conducted per RCP- CO_2 scenario. In a previous study with the aDGVM at regional scale, more than 60% of replicate simulations agreed with respect to biome projections for the year 2100 for large parts of the simulated area, the Limpopo province in South Africa (Scheiter et al., 2018). As opposed to Scheiter et al. (2018), the use of daily climate input data for our simulations helped to avoid the generation of daily climate time series with the aDGVM and thus removed the associated stochasticity. In addition, the high spatial resolution of our simulations effectively acts as a replication in space with smooth simulation

patterns in space indicating low aDGVM-caused variability in the simulation.

2.4 | Analysis of simulation results

Aboveground carbon dynamics and plant-physiological effects of eCO₂ were analysed in more detail. We defined stand WUE as the ratio of NPP and plant transpiration, following the definition by De Kauwe et al. (2013) for FACE results. We used NPP, transpiration and WUE to isolate which processes—CO₂ fertilization of photosynthesis or increased WUE via reduced transpiration through reduced g_s—are driving plant-physiological responses to eCO₂.

We created time series for total aboveground carbon and WUE in Africa for the four RCP-CO₂-scenario combinations (RCP4.5/8.5 with fCO₂/eCO₂) with annual time steps for 2000–2099. We used the ensemble mean and standard deviation (SD) of the six ensemble members for each of the four scenario combinations in each year. For other analyses, model results were averaged over 20-year periods to focus on long-term climate-driven trends (Stocker et al., 2013) and to reduce the influence of model-inherent stochastic processes on model output. Two time windows were used for comparison: 2000–2019 and 2080–2099. Maps of aboveground biomass were generated, based on the mean across all 24 simulation runs in 2000–2019, because the different scenarios did not deviate much from another. For 2080–2099, we used the ensemble mean of each of the four scenarios. In addition, changes in mean aboveground biomass from the present (2000–2019) until 2080–2099 were mapped for the four scenarios.

For changes in total aboveground vegetation carbon and in WUE (from 2000–2019 to 2080–2099), we used the omega squared (ω^2) measure to quantify the effect size of explanatory variables (see Supporting Information S1 for R code; R Core Team, 2015). CO₂ scenario, RCP scenario, and GCM and their two-way interactions were used to explain differences of the dependent variables. Using ω^2 to estimate the proportion of variance explained (Olejnik & Algina, 2003), we quantitatively evaluate the magnitude of the differences between the ensemble members (White et al., 2014). As computational limitations restricted us from implementing replicate runs, analysing for three-way interactions between the three explanatory variables was not possible.

To study potential future biome distributions and biome changes, we classified the simulated vegetation into seven biome types: desert, C₃ grassland, C₄ grassland, C₃ savanna, C₄ savanna, woodland and forest. The classification scheme is based on simulated tree cover, grass biomass and composition of tree and grass types (Scheiter et al., 2012) with minimum grass biomass levels for grassland classifications (Scheiter et al., 2018; see Table S2). In this definition scheme, the main difference between savannas and woodlands is the predominance of savanna or forest tree types, which is in turn an indicator of fire activity.

Based on this biome classification scheme, we identified biomes for the above-listed time periods for Africa for each RCP-CO₂-scenario (RCP4.5/8.5 with eCO₂/fCO₂). The biomes identified for all

GCM simulations per scenario were used to derive consensus biome maps for each scenario. For each grid cell, the biome type that was most common in the ensemble member maps was used to derive each scenario's consensus biome. According to the binomial distribution, two ensemble members agreeing in the simulated biome do not have a higher probability than an outcome by chance. Such grid cells therefore were denominated as having 'No consensus'. In addition, we plotted the number of ensemble members that simulated the consensus vegetation type for each time period as an indicator of agreement within the simulated ensemble.

We used the number of ensemble members per RCP-CO₂-scenario combination that showed a biome change from 2000–2019 to 2080–2099 (maximum six ensemble members) as an indicator for the probability of biome change under future climatic conditions. We therefore derived a measure of uncertainty from the number of simulated biome changes within a scenario. The type of biome change, that is, whether ensemble members simulate the same or different biome transitions, was not considered in this uncertainty assessment.

To illustrate the overall potential consequences (i.e. areal increase or decrease) of biome changes for each biome type, we determined each biome's change in total area covered [%] between 2000–2019 and 2080–2099 based on the consensus biome maps for all four scenarios. In addition, we plotted the changes in total area covered by each biome type for two time steps (2000–2019, 2080–2099).

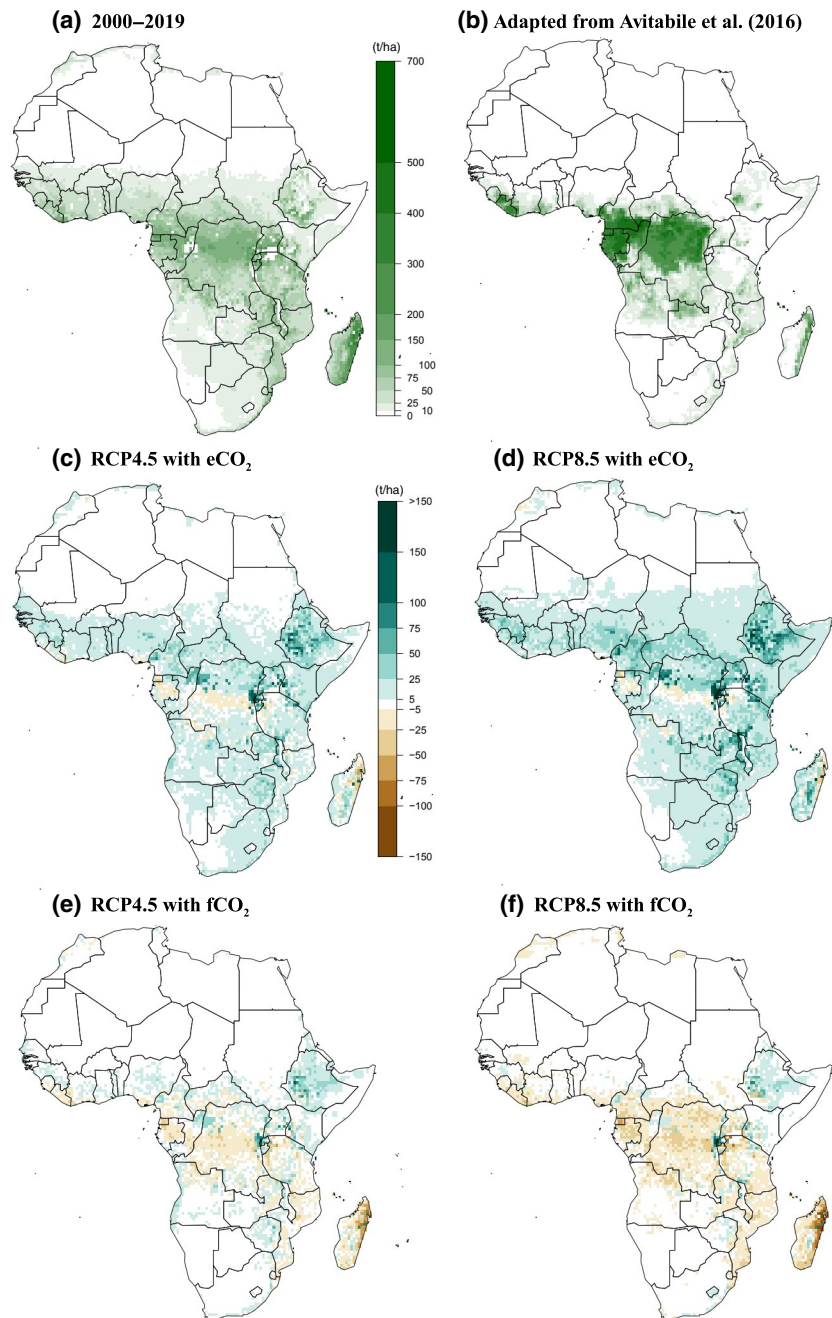
Atmospheric CO₂ effects on WUE and g_s were analysed for each RCP-CO₂ scenario, based on the relative change of ensemble means from 2000–2019 to 2080–2099 for each grid cell. As a proxy for water availability, NPP change and MAP change were plotted against each other as relative change for each RCP-CO₂ scenario combination. NPP change against tree biomass change per grid cell was used to illustrate possible effects of population dynamics on biomass. For these figures, biomes in 2000–2019 were depicted on a per grid cell basis to assess different responses for different biomes.

3 | RESULTS

3.1 | Current aboveground biomass and future projections

The spatial pattern of simulated biomass in 2000–2019 compared reasonably well with an observation-based biomass distribution (Avitabile et al., 2016; Figure 1a,b). Our simulations of potential natural biomass underestimated the high aboveground biomass in the Congo basin, while overestimating biomass in areas more distant to the equator (Figure 1a). While Avitabile et al.'s (2016) map included both intact and nonintact vegetation, aDGVM only simulated PNV, thus intact vegetation. aDGVM, therefore, overestimated simulated biomass and actual carbon stocks in areas of high land use, such as agricultural land. The mean carbon stored in simulated total aboveground biomass for Africa between 2000 and 2010 amounted to 52.2 Pg C (± 0.36 , all 24 ensemble members, Figure 2a). This is within the range of estimates derived from satellite and inventory

FIGURE 1 Simulated and observation-derived aboveground biomass in Africa and simulated change in biomass. Current aboveground biomass in Africa (t/ha) is derived from the ensemble mean across all 24 ensemble members of aDGVM-simulated biomass (2000–2019, a) and Avitabile et al. (2016, b). Change in aboveground biomass between 2000–2019 and 2080–2099 under RCP4.5 and 8.5 with eCO₂ (c, d) and with fCO₂ (e, f) is based on the mean of all six ensemble members of the respective scenario. aDGVM, adaptive Dynamic Global Vegetation Model; eCO₂, elevated CO₂; fCO₂, CO₂ fixed at 400 ppm; RCP, representative concentration pathway



plot data (48.3–64.5 Pg C; Figure 2a; Avitabile et al., 2016, Baccini et al., 2012; Liu et al., 2015; Saatchi et al., 2011; extent varies from tropical Africa to continental Africa).

When comparing current (2000–2019) and future (2080–2099) aboveground biomass, both RCP-eCO₂ scenarios showed similar spatial patterns of increasing and decreasing biomass, but areas with increasing biomass predominated (Figure 1c,d; Figure S2a,b; Table 1). Both RCP-eCO₂ scenarios showed small biomass decreases in a narrow belt along the equator. North and south of the equator both RCP scenarios showed a general pattern towards woody encroachment, with higher biomass increases for RCP8.5.

Spatial patterns of biomass change in the fCO₂ scenarios were more variable. Increases prevailed over decreases under RCP4.5 and

decreases prevailed under RCP8.5 (Table 1; Figure 1c–f). The Ethiopian Highlands were the only larger area that showed mean biomass increases for all four RCP-CO₂ scenarios. However, these increases were weaker under fCO₂ than under eCO₂. This biomass increase is in line with precipitation increases predicted for this region (Figure S1).

Both RCP-eCO₂ scenarios showed an appreciable carbon sink for Africa by the end of the 21st century in all GCM simulations (Figure 2a; Figure S3). The increase under RCP8.5 was more pronounced, whereas under RCP4.5 mean total aboveground carbon started to saturate towards the end of the century (81.3 and 70.0 Pg C in 2080–2099, respectively, see Table 2 for % change). Saturating biomass increases under RCP4.5-eCO₂ followed the projected mid-century peak in greenhouse gas emissions for RCP4.5 (Stocker

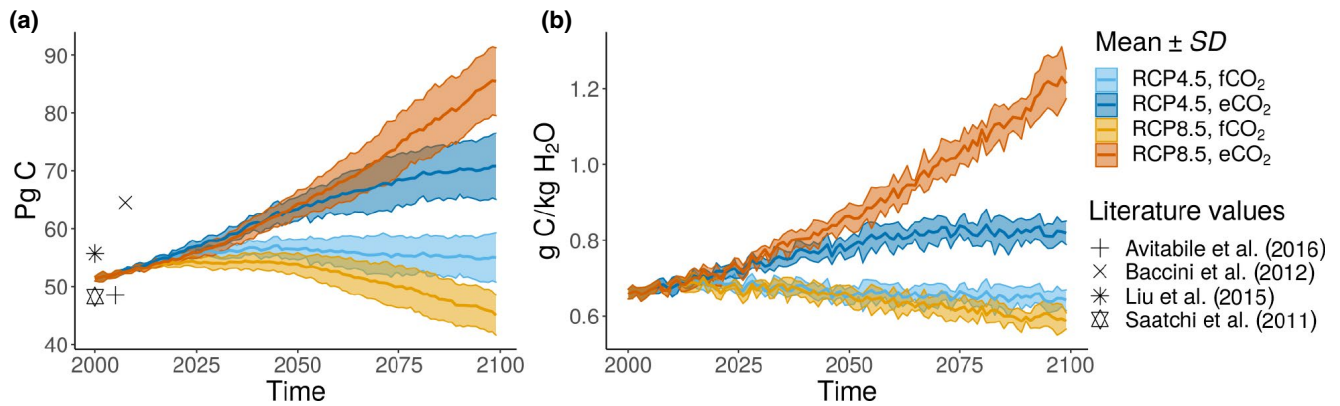


FIGURE 2 Mean total aboveground carbon and WUE in Africa in 2000–2099 under RCP4.5 and RCP8.5 with eCO₂ and fCO₂ simulated by the aDGVM. Thick lines are the mean over all six ensemble members per scenario. Shaded areas are the mean \pm standard deviation (SD) of the six ensemble members per scenario. In (a), aboveground carbon for tropical Africa (64.5 Pg C, Baccini et al., 2012), sub-Saharan Africa (48.5 Pg C, assuming 50% carbon content in aboveground biomass for Avitabile et al., 2016, and 48.3 Pg C, Saatchi et al., 2011) and Africa (55.7 Pg C, Liu et al., 2015) are depicted for comparison. See Figure S3 for aboveground carbon time series of all individual ensemble members. Water use efficiency (WUE, b) is defined as the ratio of net primary production and transpiration. See Table S3 for more details on the variability of aboveground carbon and WUE in 2080–2099. aDGVM, adaptive Dynamic Global Vegetation Model; eCO₂, elevated CO₂; fCO₂, CO₂ fixed at 400 ppm; RCP, representative concentration pathway

TABLE 1 Area (%) of Africa affected by biomass change and biome change between 2000–2019 and 2080–2099 and agreement of simulation results per scenario. Change for aboveground biomass (AGB) is given as the percentage of area with AGB increases or decreases. Where AGB increases and decreases did not sum to 100%, the remaining percentage of land area did not experience AGB changes. For biome change, proportions of area with no consensus biome in either period were not included. For agreement of biome state, only areas where all six ensemble members of a scenario agreed on simulated biome in 2080–2099 were included. The respective percentages refer to the total area of the African continent

Scenario	% area with AGB increase	% area with AGB decrease	% area with biome changes	% area with agreement in biome state in all ensemble members in 2080–2099
RCP4.5, eCO ₂	84.3	15.3	23.4	45.6
RCP8.5, eCO ₂	80.2	19.1	27.7	45.7
RCP4.5, fCO ₂	64.5	35.2	17.5	50.3
RCP8.5, fCO ₂	31.8	67.5	18.6	53.7

AGB, aboveground biomass; eCO₂, elevated CO₂; fCO₂, CO₂ fixed at 400 ppm; RCP, representative concentration pathway

TABLE 2 Change in aboveground biomass (AGB) and in WUE from 2000–2019 to 2080–2099. Change in carbon in AGB was calculated for all six ensemble members for each RCP-CO₂ scenario. The range of minimum and maximum change rate for the six ensemble members for each scenario are presented here. See Table S4 for change rates for each ensemble member

Scenario	AGB change	WUE change
RCP4.5, eCO ₂	18 to 43%	15 to 25%
RCP8.5, eCO ₂	37 to 61%	61 to 74%
RCP4.5, fCO ₂	-8 to -11%	-1 to -9%
RCP8.5, fCO ₂	-6 to -22%	-9 to -16%

AGB, aboveground biomass; eCO₂, elevated CO₂; fCO₂, CO₂ fixed at 400 ppm; RCP, representative concentration pathway; WUE, water use efficiency

et al., 2013). Variability within each RCP ensemble due to differences between the six GCMs (\pm SD, $2 \times$ SD = 9.7 and 11.2 Pg C, respectively for RCPs 4.5 and 8.5) was similar to the difference of the means of the two eCO₂ RCP scenarios (11.2 Pg C, see Table S3).

Under fCO₂, simulated total biomass in 2099 was lower than under eCO₂ (Figure 2a). For RCP8.5 under fCO₂, vegetation became a carbon source by the 2050s and biomass in 2080–2099 (47.1 Pg C, see Table 2 for % change) was less than that in 2000. For RCP4.5-fCO₂, the ensemble mean biomass in 2080–2099 was 55.2 Pg C. It depended on the downscaled GCM whether a small source or a small sink was projected for RCP4.5 under fCO₂ (Figure S3). The ω^2 metric indicated that variation in total carbon between all 24 ensemble members was mainly explained by the CO₂ scenarios, followed by interaction effects of CO₂ and RCP scenarios (Table 3; see Table S5 for corresponding F-values from ANOVA).

3.2 | Future projections of WUE and underlying plant-physiological processes

Changes in WUE, here defined as the ratio of NPP and transpiration, until 2080–2099 were similar to the trends simulated for aboveground

TABLE 3 Effect size of explanatory variables for change in carbon stored in aboveground biomass and WUE between 2000–2019 and 2080–2099. The table presents ω^2 for the dependent variables aboveground biomass change (in Pg C) and WUE change (in gC/kgH₂O) and explanatory variables CO₂ scenario, RCP scenario and GCM. Two-way interaction effects are included in the model and are denoted with ‘:’

Independent variables and interaction effects	ω^2	
	AGB	WUE
CO ₂	0.794	0.692
RCP	0.005	0.105
GCM	0.069	0.009
RCP:CO ₂	0.123	0.190
CO ₂ :GCM	0.002	0.000
GCM:RCP	0.005	0.000

AGB, aboveground biomass; GCM, general circulation model; RCP, representative concentration pathway; WUE, water use efficiency

biomass for all four RCP-CO₂ scenarios (Figure 2b; Table 2). Yet, under RCP4.5-eCO₂, WUE levelled off earlier than carbon in aboveground biomass. Both fCO₂ scenarios showed a decrease in mean WUE. For NPP and WUE, the shape of the time series was almost identical for each individual scenario (Figure 2b; Figure S4a). For transpiration on the other hand, all four scenarios showed increases (Figure S4b). Within an RCP, transpiration was lower for fCO₂ than for eCO₂.

WUE increased in most of the simulated grid cells between 2000–2019 and 2080–2099 in eCO₂ simulations, and relative change ratios were higher than in fCO₂ simulations (Figure 3a). With a stronger decrease under eCO₂ than fCO₂ and for RCP8.5 than for RCP4.5, g_s showed the opposite trend (Figure 3b). Although g_s decreased with increasing [CO₂], transpiration increased for all four RCP-CO₂ scenarios (Figure S4b). NPP was more sensitive to MAP changes under RCP8.5 than RCP4.5, with a steeper slope for eCO₂ (Figure 3c). We found increased NPP in both eCO₂ scenarios even for grid cells where MAP decreased. Variation in WUE was largely explained by the CO₂ scenario. The interaction effect between the CO₂ scenario and the RCP scenario, as well as the RCP scenario on its own also explain some of the variation (Table 3). The effect of RCP scenario on WUE was stronger than its effect on carbon in aboveground biomass.

3.3 | Projected biome changes and population dynamics

For all 24 ensemble members, aDGVM simulated biome shifts (change of spatial location of biomes) and biome transitions (change of biome type at a given location) from 2000–2019 to 2080–2099 (Figures 4 and 5 for RCP8.5 and Figures S6 and S7 for RCP4.5). This implied considerable changes in area covered by each biome (Figure 6).

Under eCO₂, in line with simulated biomass increase, biome transitions from non-woody biomes to woody biomes dominated for both RCP scenarios (Figure 4). The area covered by forest increased for

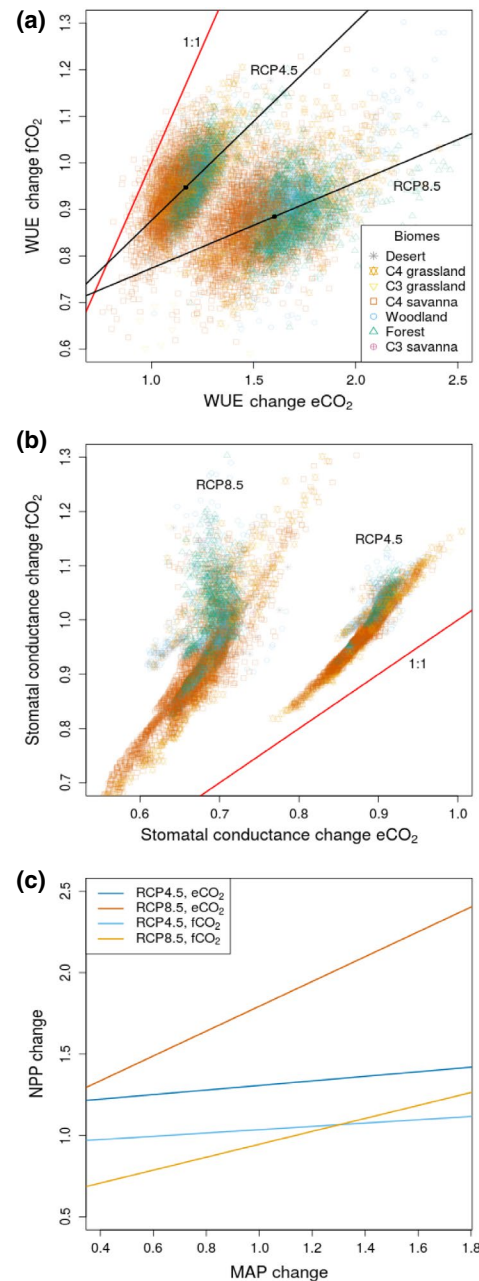


FIGURE 3 Change in WUE (a) and stomatal conductance g_s (b) under eCO₂ and fCO₂, and change in NPP versus change in MAP (continental scale, c) between 2000–2019 and 2080–2099 simulated by the aDGVM. Changes are represented by the ratio between values for 2000–2019 and 2080–2099 for each simulated grid cell. Values greater than 1 indicate an increase, values less than 1 indicate a decrease. Black lines in (a) are linear regressions for the respective RCP scenarios with the continental-scale mean of the scenario shown as a black point. Red lines represent the 1:1 lines. Each point represents a grid cell and is shape- and colour-coded according to its assigned biome type in 2000–2019. Lines in (c) are continental-scale regression lines for the four RCP-CO₂ scenario combinations. See Figure S5 for data points used to derive the MAP-NPP change regression lines for each scenario. Note that x- and y-axes do not have the same scale. aDGVM, adaptive Dynamic Global Vegetation Model; eCO₂, elevated CO₂; fCO₂, CO₂ fixed at 400 ppm; MAP, mean annual precipitation; NPP, net primary production; RCP, representative concentration pathway; WUE, water use efficiency

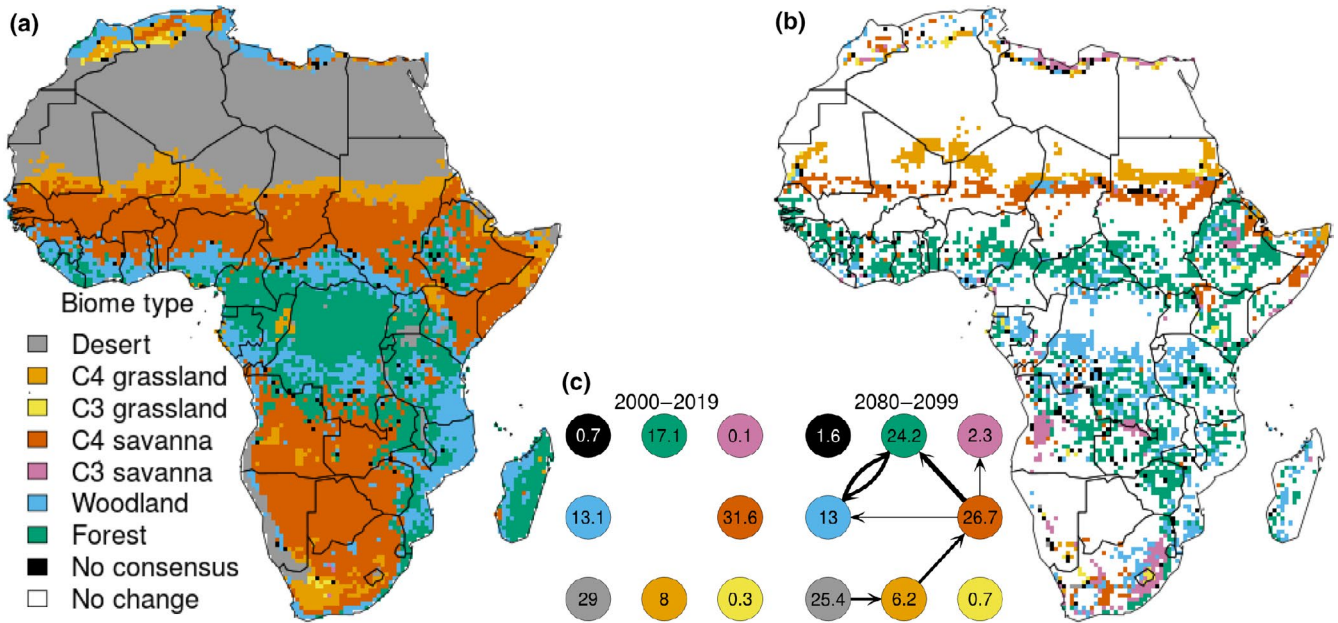


FIGURE 4 Consensus biome type under RCP8.5-eCO₂ in 2000-2019 (a), biome changes until 2080-2099 (b) and transitions and fractional cover of biomes (c) simulated by aDGVM. The consensus biome type is the biome simulated by at least three ensemble members of the scenario. Grid cells with an agreement of less than three ensemble members do not have a higher probability than an outcome by chance and are marked as ‘No consensus’. The biomes shown in (b) are the biomes that were simulated for 2080-2099 for grid cells where biome transitions were simulated for the consensus biome. Numbers in each coloured circle (c) represent the percentage of area covered by each biome at the respective time step in the consensus map. Arrows show biome changes with regard to the previous time step. Arrow thickness is proportional to the change in total area. In panel (c), only changes that affected more than 0.5% of the African land surface are shown. See Figure S6 for RCP4.5-eCO₂, aDGVM, adaptive Dynamic Global Vegetation Model; eCO₂, elevated CO₂; RCP, representative concentration pathway

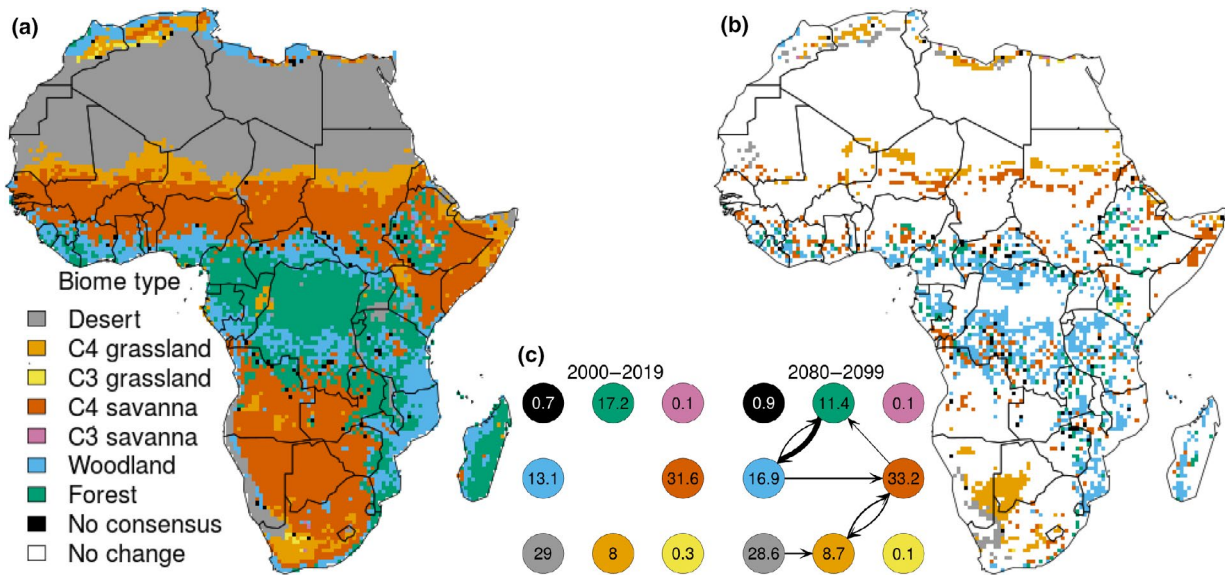


FIGURE 5 Consensus biome type under RCP8.5-fCO₂ in 2000-2019 (a), biome changes until 2080-2099 (b) and transitions and fractional cover of biomes (c) simulated by aDGVM. The consensus biome type is the biome simulated by at least three ensemble members of the scenario. Grid cells with an agreement of less than three ensemble members do not have a higher probability than an outcome by chance and are marked as ‘No consensus’. The biomes shown in (b) are the biomes that were simulated for 2080-2099 for grid cells where biome transitions were simulated for the consensus biome. Numbers in each coloured circle (c) represent the percentage of area covered by each biome at the respective time step in the consensus map. Arrows show biome changes with regard to the previous time step. Arrow thickness is proportional to the change in total area. In panel (c), only changes that affected more than 0.5% of the African land surface are shown. See Figure S7 for RCP4.5-fCO₂, aDGVM, adaptive Dynamic Global Vegetation Model; fCO₂, CO₂ fixed at 400 ppm; RCP, representative concentration pathway

FIGURE 6 Change in African area covered by each biome in each GCM simulation and ensemble medians (box plots) under RCP4.5 and RCP8.5 with eCO_2 and fCO_2 simulated by aDGVM. Change is the difference in area covered between the time periods 2000–2019 and 2080–2099 in percentage points (left axis) and km^2 (right axis). aDGVM, adaptive Dynamic Global Vegetation Model; eCO_2 , elevated CO_2 ; fCO_2 , CO_2 fixed at 400 ppm; GCM, general circulation model; RCP, representative concentration pathway

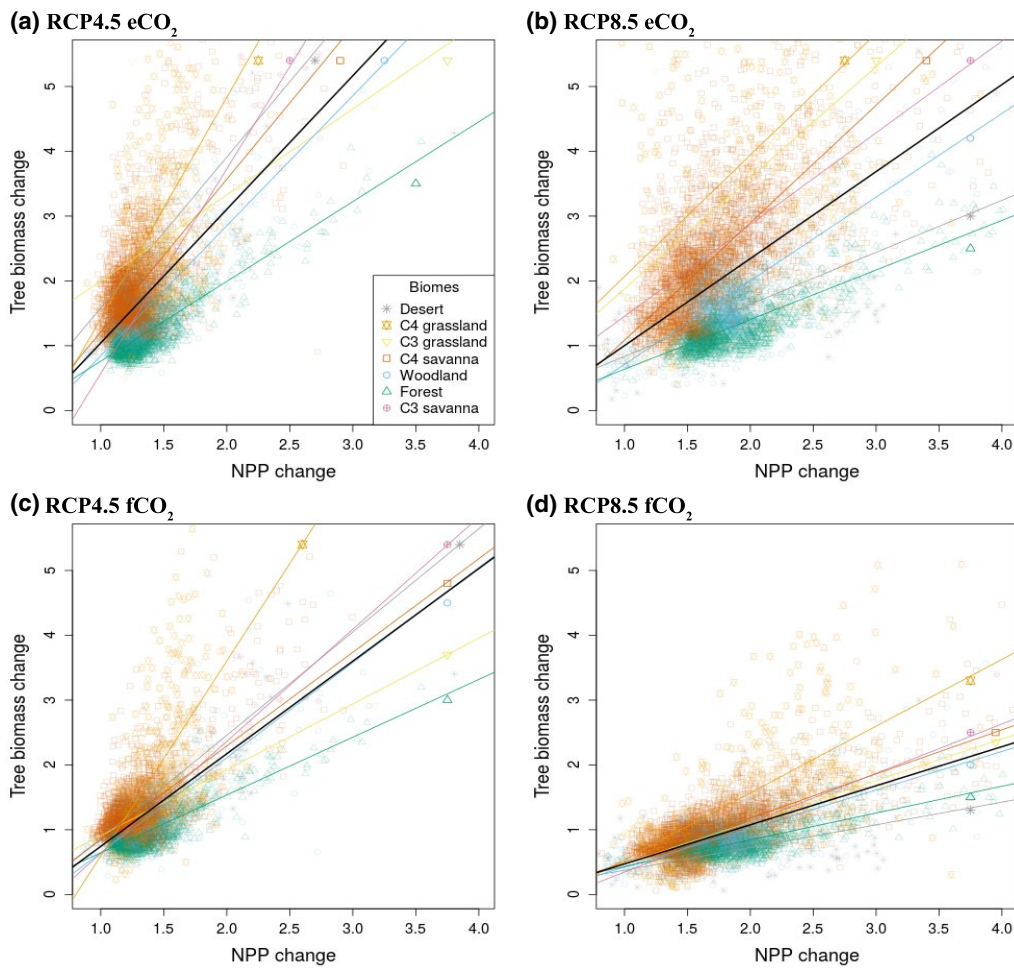
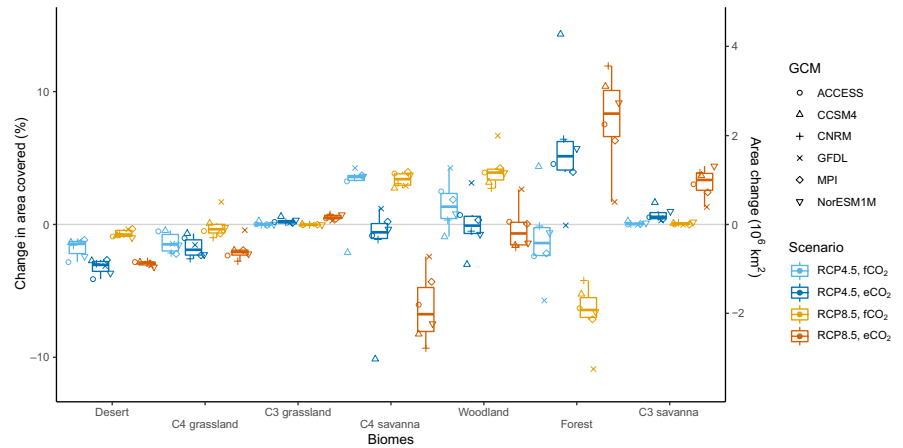


FIGURE 7 Mean tree biomass change in relation to mean NPP change for eCO_2 (a, b) and fCO_2 (c, d) under RCP4.5 (a, c) and RCP8.5 (b, d) simulated by aDGVM. Change is represented by the ratio between 2000–2019 and 2080–2099. Hence, values greater than 1 indicate increase and values less than 1 indicate decrease. Black lines are regression lines for all data points of the mean of a scenario. Coloured lines are regression lines for the respective biomes in 2000–2019 of the mean of a scenario. The regression lines for biomes are marked with a symbol at the top right of each line with colour and shape of the respective biome. Each point represents the mean for a simulated grid cell, and colour and shape represent the grid cell's consensus biome type in 2000–2019. The mean of each scenario is based on the six GCM simulations in each time period. Note that the scales of x- and y-axes differ. aDGVM, adaptive Dynamic Global Vegetation Model; eCO_2 , elevated CO_2 ; fCO_2 , CO_2 fixed at 400 ppm; GCM, general circulation model; NPP, net primary production; RCP, representative concentration pathway

both RCP- eCO_2 scenarios at the expense of desert, grasslands and savannas, with stronger effects for RCP8.5 (Figure 6). Non-desert biomes shifted towards mid-latitudes (Figure 4a,b; Figure S6a,b).

However, in line with simulated biomass reductions, woodland replaced forests in some areas close to the equator (Figure 1c,d). [CO_2] increase and climatic change are stronger in RCP8.5, therefore the

aDGVM simulated that larger areas changed biome state than under RCP4.5 (Table 1). Large areas showed transitions from C_4 savanna to forest, especially under RCP8.5 (Figure 4c).

As opposed to the eCO_2 scenarios, a decrease in forests dominated biome cover changes in the fCO_2 scenarios (Figure 5). In total, under fCO_2 , a smaller area was projected to experience biome transitions (Table 1). For RCP8.5, we found a strong decrease in forest cover (5.8 percentage points) and an increase in C_4 -dominated biomes. Forests mainly changed to woodlands in both RCP scenarios (Figure 5c; Figure S7c). Under RCP8.5- fCO_2 , the core savanna area in 2080–2099 in southern Africa was smaller and located further north than in the other three scenarios (Figures S8e,f and S9e,f), with a pronounced transition from C_4 savanna to C_4 grasslands in the Kalahari region (Figure 5a,b). Under RCP4.5, the cover fractions of biome types did not change as much, with transitions in favour of C_4 savanna and woodlands.

Rates of tree biomass change were biome specific and varied between CO_2 scenarios (Figure 7). Under eCO_2 , C_4 savannas showed a stronger relative increase in tree biomass change rates than woodlands and forests for both RCP scenarios, hinting at population dynamic effects (Figure 7a,b). Tree biomass change in C_4 savannas was more sensitive to NPP change than in other woody biomes for both eCO_2 scenarios. With fCO_2 , an increase in NPP often did not lead to an increase in tree biomass, especially for RCP8.5 and forest biomes.

3.4 | Uncertainty of biome projections

The simulated biomes for the six ensemble members of all four RCP- CO_2 scenarios agreed well at the beginning of the simulations

(2000–2019) in the equatorial forests, the Sahara desert along the Tropic of Cancer, and in more open C_4 savanna areas (Figure 8a; Figure S10a). In the transition zones between these biome types, the ensemble members agreed less well and agreement was low in grasslands, closed savannas and woodlands.

Agreement of the six ensemble members per scenario decreased towards the end of the 21st century, especially for eCO_2 scenarios (Figure 8b,c; Figure S10b,c). The core areas of forest, C_4 savanna and desert, where all six ensemble members still showed high agreement within a scenario, decreased. Agreement was higher for fCO_2 scenarios, where only climate change influenced vegetation changes (Table 1; Figure 8b,c; Figure S10b,c).

Under eCO_2 , the projections for the transition zones between forest and C_4 savanna, and C_4 savanna and desert showed increasing disagreement between ensemble members for each RCP scenario (Figure 8b; Figure S10b), with the desert–grassland–savanna transition zone north of the equator at a medium to high probability of biome transition in our simulations, especially under RCP8.5 (Figure 9a; Figure S11a). Further hotspots of medium to high probability of biome transitions for both RCP- eCO_2 scenarios were found in eastern Africa, areas north and south of the equator in the humid and moist subhumid tropics, and for RCP8.5 in southern Africa with an increased dominance of C_3 plants (Figures 4b and 9a).

In fCO_2 scenarios, biomes were projected to have a lower probability of change (Figure 9b; Figure S11b). The hotspot of likely biome transitions south of the equator under eCO_2 was also simulated under fCO_2 for both RCP scenarios. Conversely, unlike in the eCO_2 scenarios, the southern Kalahari was projected to change with medium to high probability under RCP8.5- fCO_2 . Overall for both CO_2

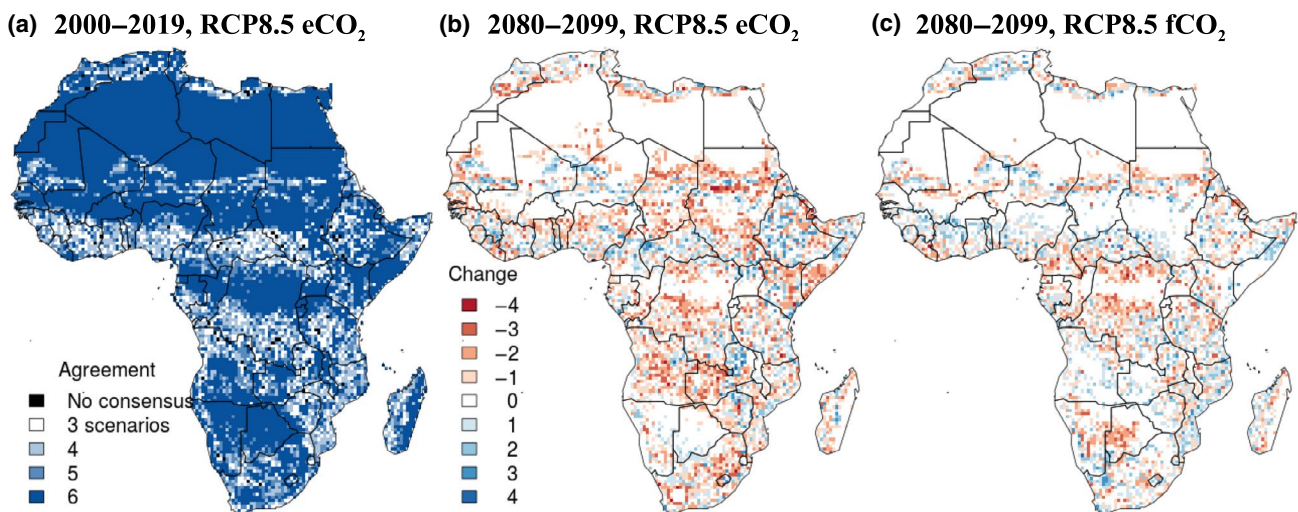


FIGURE 8 Agreement of ensemble members in 2000–2019, under eCO_2 (a) and change in agreement until 2080–2099 under eCO_2 (b) and fCO_2 (c) for RCP8.5 in aDGVM simulations. The number of ensemble members simulating the consensus type is denoted as 'Agreement'. Grid cells with an agreement of less than three ensemble members are marked as 'No consensus'. We only displayed the number of ensemble members simulating the consensus type in 2000–2019 for eCO_2 in (a), because agreement is almost identical for eCO_2 and fCO_2 (see Figures S8b and S9b). The consensus biome type is the biome simulated by at least three ensemble members of the scenario. See Figure S10 for RCP4.5. aDGVM, adaptive Dynamic Global Vegetation Model; eCO_2 , elevated CO_2 ; fCO_2 , CO_2 fixed at 400 ppm; RCP, representative concentration pathway

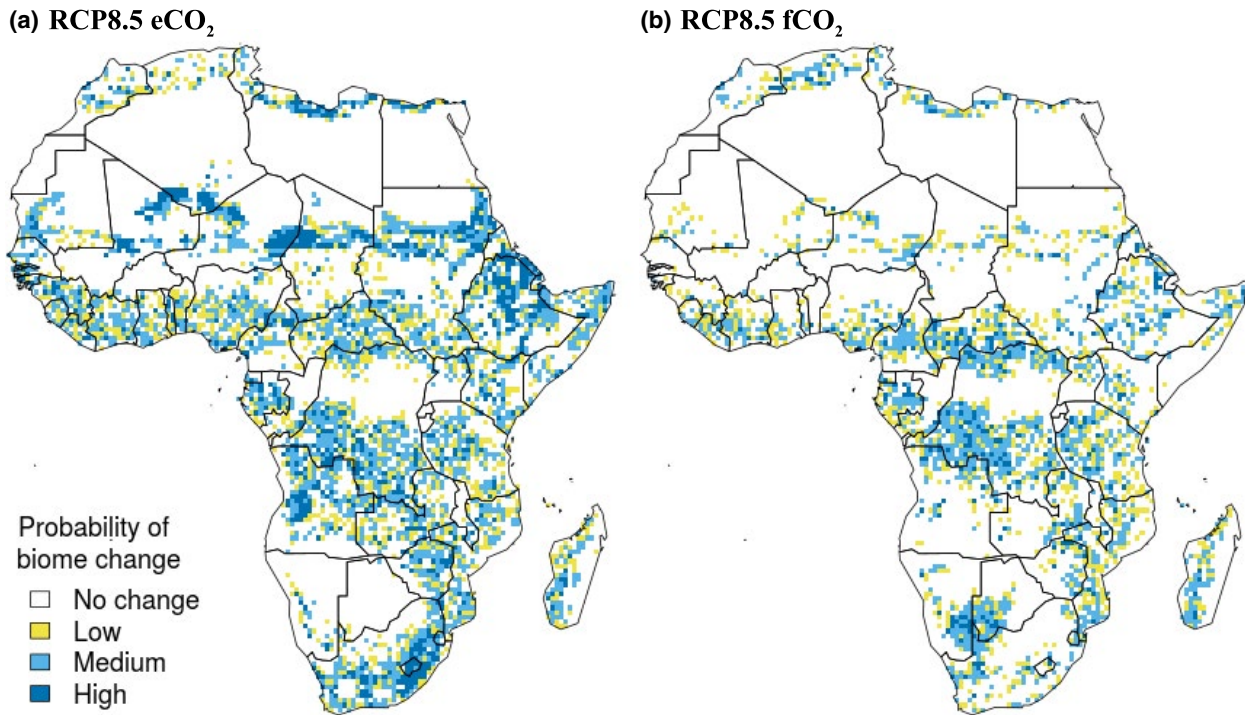


FIGURE 9 Probability of biome change between 2000–2019 and 2080–2099 simulated by aDGVM. The proportion of the six GCM ensemble members per scenario—here RCP8.5, eCO₂ (a) and fCO₂ (b)—that showed a biome change from 2000–2019 to 2080–2099 was used as a measure of probability of biome change. The more ensemble members projected a biome change per grid cell, the higher its probability of biome change. High probability of biome change—all six simulations project biome changes; medium probability of biome change—four or five simulations with biome changes; low probability of biome change—three simulations with biome changes; no change—zero to two simulations with changes. Grid cells with two or fewer simulations with biome changes do not have a higher probability than an outcome by chance and were therefore regarded as ‘No change’. Whether the ensemble members simulated the same type of biome transition was not considered here. See Figure S11 for RCP4.5. aDGVM, adaptive Dynamic Global Vegetation Model; eCO₂, elevated CO₂; fCO₂, CO₂ fixed at 400 ppm; GCM, general circulation model; RCP, representative concentration pathway

scenarios, under RCP8.5, a larger area in Africa had a medium to high probability for biome transitions than under RCP4.5 (Figure 9; Figure S11).

4 | DISCUSSION

The aim of this study was to provide projections of climate- and [CO₂]-driven vegetation changes in Africa until the end of the century using a regionally adapted DGVM and regionally downscaled climate data. We analysed plant-physiological and vegetation dynamic responses to eCO₂ and quantified the impact of three sources of uncertainty on vegetation projections: the influence of climate models (GCM implementations), future global socio-economic development (RCP scenarios) and strength of CO₂ effects on plant growth (CO₂ scenarios).

We found that large regions in Africa are likely to experience changes in biomes and carbon stocks, especially with eCO₂ response scenarios. The extent of the projected changes depended on the chosen scenario and patterns were less clear for biome changes. Projected change in aboveground biomass was driven primarily by CO₂ fertilization and showed that assumptions concerning CO₂ effects (eCO₂ or fCO₂) caused the strongest variability in future projections (Table 3; Figure 2; Figure S3). Even medium-impact

scenarios (RCP4.5, irrespective of CO₂ scenario) suggested considerable ecosystem change (Figure 6; Figure S6b,c).

4.1 | Plant-physiological effects of eCO₂ and drivers of woody encroachment

Elevated CO₂ led to strong woody encroachment in our projections and was accompanied by enhanced WUE. Increases in NPP clearly drove WUE enhancement, although both photosynthesis (increase in NPP via more efficient CO₂ fixation) and *g_s* (decrease) are affected by eCO₂ in aDGVM. We therefore conclude that increased WUE, intensification of carbon sinks and woody encroachment are mainly driven by CO₂ fertilization of photosynthesis in aDGVM. This finding seems to contradict observational studies that found that increased intrinsic WUE in mature tropical and subtropical trees did not translate into growth enhancement and often even resulted in declining tree growth rates (Peñuelas et al., 2011; Silva & Anand, 2013; van der Sleen et al., 2015). However, our simulated biomass increases in savannas are driven by a combination of demographic processes and CO₂ fertilization effects on tree seedlings and saplings, which are submature, unlike most empirical studies (Figure 7).

Similar to observations reported from FACE experiments in young forest stands (Warren et al., 2011), the effects of increased NPP and vegetation cover on transpiration outweigh the effects of decreased g_s under eCO_2 with increased transpiration having a dampening effect on WUE. For RCP8.5, this leads to an increased positive relation between NPP and MAP change with a steeper slope under eCO_2 . The increased sensitivity of NPP to MAP under RCP8.5 implies stronger limitation of plant growth by soil moisture availability. This limitation is driven by a combination of higher demand for water by more productive vegetation, higher transpiration (Figure S4b), temperature increases and regionally decreasing MAP (Figure S1). However, the g_s model implemented in the aDGVM might not represent eCO_2 responses adequately in these increasingly water-limited ecosystems (Medlyn et al., 2001).

Our results confirm results from previous DGVM studies that plant-physiological CO_2 effects strongly impact projections of future vegetation states (Cramer et al., 2001; Hickler et al., 2015; Huntingford et al., 2013; Rammig et al., 2010; Sato & Ise, 2012). The ensemble modelling results are useful to estimate potential lower and upper bounds of potential eCO_2 effects. Disabled eCO_2 effect scenarios serve as a surrogate for low physiological sensitivity of plants to eCO_2 and represent an artificial lower bound of change. It is, however, unlikely that eCO_2 effects on plants will be negligible in systems composed of C_3 and C_4 plants, where feedbacks between CO_2 fertilization and fire disturbance affecting the competitive balance between C_3 and C_4 plants have been postulated (Midgley & Bond, 2015). However, DGVMs such as aDGVM might not adequately represent carbon sink–source processes and other non-photosynthetic growth limitations (Körner, 2015), though empirical work by Kgope et al. (2010) strongly implicate sink–source effects in controlling the demographic process under elevated CO_2 , as simulated by aDGVM. The first submodels that consider long-term physiological acclimation effects in plants to eCO_2 are now being implemented in DGVMs (Haverd et al., 2018).

Nutrient dynamics in plants and ecosystems can stimulate or reduce eCO_2 effects on plants, but are not represented in aDGVM. Low nutrient availability, for example, nitrogen and phosphorus deficits, limits the growth-enhancing effects of eCO_2 and therefore on aboveground biomass (e.g. Jiang, Caldararu, et al., 2020; Peñuelas et al., 2011). Vegetation models including nutrient cycling frequently predict smaller eCO_2 effects (Fleischer et al., 2019; Hickler et al., 2015). Field data suggest that tree encroachment might further reduce nitrogen availability in African savannas, which might lead to a negative feedback on CO_2 -induced tree encroachment (Higgins et al., 2015). The ability of trees to benefit from eCO_2 under nutrient limitation depends on their association with different mycorrhizal types and a tree's ability to fix atmospheric nitrogen (Terrer et al., 2018) with nitrogen-fixing trees from the Fabaceae family having high abundances in African savannas (Stevens et al., 2017). Under nitrogen limitation, tree species associated with arbuscular mycorrhizae, the dominant type in the tropics, benefit less than trees associated with ectomycorrhizae or N_2 fixers (Terrer et al., 2016, 2018).

Based on extrapolation of 138 eCO_2 experiments, Terrer et al. (2019) confirmed substantial biomass increases due to CO_2 fertilization in past decades and likely in the future, even when accounting for nutrient limitation. They estimated $12 \pm 3\%$ and $12.5 \pm 3\%$ increases in global and tropical biomass, respectively, as a result of a 250 ppm increase in $[CO_2]$ from 375 ppm by 2100. This is less than the increase of 26.9% in aDGVM-projected aboveground biomass for eCO_2 -compared to fCO_2 scenarios in 2080–2099 for RCP4.5 ($\Delta CO_2 \sim 135$ ppm, Figure 2a), but Terrer et al.'s results clearly ignore demographic effects that result in biome structural shifts. Next to missing nutrient limitations in aDGVM, another explanation for this mismatch could be that empirical eCO_2 experiments do not account for ecological feedback mechanisms proposed for savannas that might foster woody encroachment and increase biomass stocks (Midgley & Bond, 2015), nor does Terrer et al.'s meta-analysis explicitly (but indirectly) include N_2 fixation and the associated eCO_2 response. Indeed, Stevens et al. (2017) found that recent patterns of woody encroachment in savannas in Africa are often due to N-fixing species. Thus, large uncertainties in vegetation response remain with a significant response to be expected in tropical areas. For representation in DGVMs, the FUN2.0 model offers a mechanism that considers a range of processes for nitrogen acquisition (e.g. different mycorrhizal strategies, active uptake, resorption from senescing leaves; Shi et al., 2016).

Belowground carbon, including roots and soil carbon, are estimated to make up 77% of Sub-Saharan Africa's carbon stocks (161 of 209 Pg C total C stocks, Bombelli et al., 2009). We acknowledge that root biomass and soil carbon are crucial for a full representation of the terrestrial carbon cycle, especially as carbon and nitrogen cycles are highly interdependent. Soil and vegetation responses to climate change and eCO_2 may vary and may impact carbon cycling significantly (Dietzen et al., 2019; Dufresne et al., 2002).

Long-term FACE experiments in African ecosystems (such as AmazonFACE in Brazil and OzFACE in Australia; Norby et al., 2016; Stokes et al., 2005) in combination with eCO_2 experiments such as open-top chamber experiments with savanna plants (B. S. Ripley, personal communication, March 2019) may provide further insights regarding the long-term effects of eCO_2 in Africa. Consolidated results from these experiments will contribute to a comprehensive understanding of the effects of rising $[CO_2]$ on African plant communities and can be used to revise process implementation in DGVMs.

4.2 | Climate change impacts on biome patterns

Projected biome changes towards woody vegetation under eCO_2 are consistent with results from previous studies on regional (Doherty et al., 2010) and continental scale (Conradi et al., 2020; Gonzalez et al., 2010; Higgins & Scheiter, 2012; Niang et al., 2014; Scholze et al., 2006; Sitch et al., 2008). The transition of grassland and savanna biomes, that is, C_4 -dominated biomes, to more woody biomes, that is, C_3 -dominated biomes, in eCO_2 simulations corroborates findings that savannas and grasslands are particularly vulnerable to biome changes

under eCO₂ (Higgins & Scheiter, 2012; Osborne et al., 2018; Scheiter et al., 2018). Woody encroachment into grasslands and savannas in Africa is a major threat to their biodiversity (Bond, 2016).

Tropical forests are less stable in our simulations than suggested by Gonzalez et al. (2010), Scholze et al. (2006) and Sitch et al. (2008). Climatic changes outweigh eCO₂ effects in a belt south of the equator with decreasing biomass in both CO₂ scenarios by 2080–2099, which is similar to DGVM results by Sato and Ise (2012) and projections of carbon sinks saturating in African tropical forests by 2040 (Hubau et al., 2020). In our simulations, this decrease in regional carbon stocks in forests is outweighed on the continental scale by increases in other tropical forest areas as well as savanna and grassland areas that were not included in the study by Hubau et al. (2020). Feedbacks between population dynamics and combined fire-eCO₂ effects in the aDGVM also explain this discrepancy. While Hubau et al. (2020) used linear regression models both to project predictor variables, such as mean annual temperature, and then based on these to project carbon changes into the future, here the process-based aDGVM was driven with downscaled GCM data. Increases in aboveground biomass and transitions to forest biomes in East Africa under both eCO₂ and present-day [CO₂] levels (400 ppm, fCO₂) for both RCP scenarios are the result of higher water availability due to increased precipitation in these areas (Figure S1e,f; Archer et al., 2018; Doherty et al., 2010; Engelbrecht et al., 2015; Niang et al., 2014).

Large proportions of simulated biome changes under eCO₂ occur in the moist subhumid and humid tropics where woodland and C₄ savanna biomes were found in 2000–2019 (Figure 4a,b). This is opposed to previous studies where most changes occurred further north and south of the equator in regions with more open savannas (Gonzalez et al., 2010; Higgins & Scheiter, 2012).

Explanations for differences in biome change projections between different studies include the use of different modelling approaches (e.g. species distribution models, Conradi et al., 2020), different climate data sets (e.g. GCM data or interpolated data such as ISIMIP instead of RCM data), different DGVMs (Doherty et al., 2010; Gonzalez et al., 2010) and that precipitation changes until 2100 were not accounted for (Higgins & Scheiter, 2012). In addition, utilization of different biome classification schemes can influence if and where vegetation changes are simulated (Scheiter et al., 2020) and create mismatches between different vegetation models that impede comparison of simulated biomes. Nonetheless, the different studies agree on a potential increase in the area covered by woody biomes under future climatic conditions.

Where MAP decreases and temperatures increase, C₄ plants can maintain their competitive advantage over C₃ plants even under eCO₂ (Higgins & Scheiter, 2012). We found such behaviour in south-western Africa, where the CCAM ensemble predicts a decrease in MAP, and a temperature increase to levels unprecedented in recent history. Bush encroachment observed in this region in the recent past was explained by a combination of [CO₂] increase, precipitation increase and land-use practices such as livestock grazing (O'Connor et al., 2014). However, future projections of precipitation in our forcing data for this region showed a trend towards

substantial precipitation decreases, that is, opposed to increases in the past, whereas land use was not considered in our study. In particular, the shift from C₄ savanna to C₄ grasslands by 2080–2099 in the Kalahari under RCP8.5 with fCO₂ is due to the competitive advantage of C₄ plants over C₃ trees under drier conditions at lower [CO₂]. Differences between Higgins and Scheiter's (2012) and our result in this region illustrate that it is crucial to include precipitation changes in vegetation projections under climate change. On the one hand, an increasing likelihood or severity of droughts under future climate conditions may offset the eCO₂ effect, as plant responses to eCO₂ are hampered by low soil water availability (Nowak et al., 2004; Reich et al., 2014). On the other hand, advantages of C₄ grasses over C₃ grasses in dry habitats may be reduced under drought conditions (Taylor et al., 2011).

4.3 | Uncertainties of vegetation projections

In our simulations, direct eCO₂ effects on plants are the primary determinants of the future carbon sink or source, WUE and biome states in Africa (Figures 2 and 6; Table 3). This is consistent with the results from Rammig et al. (2010) for the Amazon and Huntingford et al. (2013) for the global tropics. Direct eCO₂ effects are very likely, but considerable uncertainty remains with respect to the strength of the effect. Thus, the effect sizes in Table 3 only allow comparison of CO₂ effects and climate input data as simulated by the aDGVM. Nevertheless, our results suggest that improving our understanding of plant-physiological CO₂ effects is crucial to achieve realistic future ecosystem projections.

Areas with high uncertainty in projected biome transitions only partially agree with patterns reported by Gonzalez et al. (2010). Uncertainty is often higher in our study (Figure 9a). Both studies agree on high uncertainty for biome changes in the western parts of the transition zone between the Sahel and the Sahara. The uncertainty of biome change we inferred in this study was similar or smaller than that in Scholze et al.'s (2006) projections. Low agreement of projected biome changes in grassland, closed savanna and woodland areas in our ensemble can be explained by alternative vegetation states related to fire occurrence typical for Africa (Hoffmann et al., 2012; Moncrieff et al., 2014; Staver et al., 2011) and variability in climatic drivers derived from GCMs, in particular uncertainty regarding precipitation.

Uncertainty in future projections is increased by the interplay of eCO₂, fire and feedbacks caused by population dynamics. Enhanced tree sapling growth under eCO₂ may eventually reduce grass biomass and fine fuel availability, which in turn reduces fire frequency and intensity. In combination with climate changes, this feedback mechanism can lead to a rapid woody encroachment in savanna ecosystems (Figure 7; Midgley & Bond, 2015). Fire disturbance is a factor shaping ecosystems (e.g. Bond & Midgley, 2012; Midgley & Bond, 2015; Scheiter et al., 2012) leading to multiple stable states for the same climate zones (e.g. Higgins & Scheiter, 2012; Staver et al., 2011). Fire has been shown to influence and delay projected biome changes and can delay transitions to woody

biomes and thus stabilization of ecosystem states after changes in environmental drivers stabilized (e.g. [CO₂], Scheiter et al., 2020). Even when ecophysiological processes have already saturated (e.g. here expressed via NPP), ecosystem states continue to change (e.g. biomass, Figure 2a; Figure S4a), because they have not reached an equilibrium state under changed environmental conditions. In addition, stochastic processes in the aDGVM fire model and differences in GCM climate projections can produce varying fire occurrences in different ensemble members and thus explain uncertainty in projections, especially in fire-shaped ecosystems like savannas. Other disturbances not included here, such as herbivory, and their interactions with fire and eCO₂ are additional factors of uncertainty in vegetation projections.

Despite the uncertainties in regional patterns, the projections of substantial biome changes across all scenarios of the ensemble suggest substantial future changes in habitat structure and biodiversity. These potentially large changes in climate and biomes sharply contrast with relative stability in past climates and disturbance regimes in Africa, which probably contributed to its high biodiversity (Midgley & Bond, 2015).

4.4 | Opportunities for future ensemble vegetation simulations

By downscaling climate data from a GCM with an RCM, regional change is represented consistent with global changes, but regional features such as topography that affect regional climate are accounted for (Morales et al., 2007). Future studies could increase the ensemble size by using downscaled climate from multiple RCMs. However, Morales et al. (2007) have shown for Europe that the choice of the GCM used as boundary condition for an RCM is more important than the choice of the RCM when applying downscaled climate data in an ecosystem model. We therefore considered the CCAM ensemble in combination with the CO₂ scenarios as sufficient for this study.

Extending the ensemble by applying the same simulation design to different DGVMs would allow assessing the impact of different implementations of vegetation processes in DGVMs and the associated variability in DGVM results (Nishina et al., 2015; Sitch et al., 2008; Warszawski et al., 2014). The physiological representation in many DGVMs is based on the biochemical model of photosynthetic assimilation in leaves of C₃ and C₄ plants developed by Farquhar et al. (1980) and Collatz et al. (1991, 1992; Sitch et al., 2008). Therefore, we expect similar eCO₂ responses in an ensemble of DGVMs, unless the DGVMs additionally include nutrient limitation, or different representations of carbon allocation or of stomatal control models.

4.5 | Socio-economic development and flexible adaptation

The stronger impacts under RCP8.5 compared to RCP4.5, irrespective whether eCO₂ or fCO₂ is assumed, entail that today's decisions

from individual to policy level shape the degree to which climate, ecosystems and livelihoods will change. The strong carbon sink simulated here under RCP8.5-eCO₂ might suggest regional potential for land-based climate mitigation, but the associated conversion of grassy biomes to more encroached biomes is a threat to their biodiversity. Increased woody cover in grassy biomes might lead to losses of their ecosystem services, such as arable and range land (Bond et al., 2019; Parr et al., 2014).

The range of possible climate change impacts in Africa presented in our study can support policymakers and stakeholders in Africa in planning for alternative climate futures in climate change adaptation measures (Müller et al., 2014) even though the study was not specifically designed to address policy questions. Our PNV simulations, for example, could help to guide good practice in nature conservation and land-use planning (Loidi & Fernández-González, 2012) or to avoid afforestation activities in non-forest ecosystems (Bond et al., 2019; Brancalion et al., 2019; Veldman et al., 2015). Stakeholders such as NGOs and state agencies can use projections of PNV to raise awareness for possible climate change impacts. To inform policymakers and stakeholders, it will also be necessary to include land management practices such as livestock and fire management in model simulations (e.g. Pfeiffer et al., 2019; Scheiter & Savadogo, 2016; Scheiter et al., 2019) and to implement DGVM ensemble simulations with greenhouse gas emissions and land-use scenarios of different Shared Socio-Economic Pathways (SSPs; Popp et al., 2017).

As the large differences between the different scenarios imply large uncertainties, adaptation strategies must be highly adaptive and flexible. Over time, observations of climate change and impacts on ecosystems will provide an improved knowledge base (Fletcher et al., 2019). As opposed to using vegetation projections only, Bayesian statistics combined with a stochastic dynamic programming approach allow an upfront assessment of the opportunity of this increased knowledge base in the future (Fletcher et al., 2019; Yousefpour et al., 2012). Thus, trade-offs between investing in highly flexible measures compared to potentially simpler but less flexible measures can be weighed against each other (Fletcher et al., 2019). In combination with updated information on population developments and land-use change via continued monitoring, this method may support stakeholders in the development of adequate management plans. However, implementing this method requires close and iterative exchange between stakeholders and scientists, so that specific policy and planning questions and their uncertainties can be assessed using vegetation projections as an exploratory tool adjusted to the specific question (Weaver et al., 2013).

Combining DGVMs with land use, SSPs and population development would give deeper insights into the vulnerability of different regions in Africa to climate change. However, knowledge of PNV states is a basis for future conservation planning and provides an estimate of ecosystem and plant types that could persist and thrive under future climatic conditions. When considering human population development and future potential land use, information on PNV is essential to feed into development policies. Especially in regions with higher uncertainty regarding the impact of climate change on

future PNV, a diverse set of climate change adaptation measures needs to be included in development strategies, such as diversification of income and flexibility in production methods, to account for this uncertainty (Müller et al., 2014). Policies need to embrace the opportunities of continuous knowledge gain about climate change impacts (Fletcher et al., 2019) based on latest monitoring results, empirical research and updated models with scientists and policy-makers collaborating closely in the decision-making process.

ACKNOWLEDGEMENTS

This study and C.M. were funded under the SPACES programme (Science Partnerships for the Assessment of Complex Earth System Processes) under the German Federal Ministry of Education and Research (BMBF)'s framework programme (Project EMSAfrica, grant number 01LL1801B). M.P. thanks the BMBF SPACES initiative for funding the project South African Limpopo Landscapes Network (SALLnet, grant 01LL1802B). G.F.M. acknowledges support under a Humboldt Research Award, and funding under the NRF Global Change Grand Challenge Grant number 11859. S.S. thanks the DFG Emmy Noether programme for funding grant SCHE 1719/2-1. The authors thank the SBIK-F modelling centre research group and the ARS AfricaE and EMSAfrica research consortia for valuable insights. Open access funding enabled and organized by Projekt DEAL.

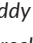


AUTHOR CONTRIBUTION

C.M., S.S. and T.H. conceived the study. C.M. designed and conducted the analysis of simulation results and led the writing of this article. S.S. conducted the simulations for this study. S.S. and T.H. contributed to the analysis of simulation results. C.D.-R. and F.E. provided the climate forcing data used in this article. G.F.M. provided valuable support for the implementation of this study. T.H., C.D.-R., F.E., S.I.H., G.P.v.M., G.F.M., M.P. and S.S. contributed to the writing of this article.

DATA AVAILABILITY STATEMENT

The aDGVM code that was used to produce the results in this publication is available on Github (https://github.com/aDGVM/aDGVM1_CCAM). aDGVM simulation results are accessible through the SASSCAL database (http://data.sasscal.org/metadata/view.php?view=li_rbis_process_step&id=6379&ident=118872017185729320).

ORCID

Carola Martens  <https://orcid.org/0000-0003-3954-039X>
 Thomas Hickler  <https://orcid.org/0000-0002-4668-7552>
 Claire Davis-Reddy  <https://orcid.org/0000-0002-8635-5691>
 Francois Engelbrecht  <https://orcid.org/0000-0002-9189-6556>
 Steven I. Higgins  <https://orcid.org/0000-0001-5695-9665>
 Graham P. von Maltitz  <https://orcid.org/0000-0002-9272-1272>
 Guy F. Midgley  <https://orcid.org/0000-0001-8264-0869>
 Mirjam Pfeiffer  <https://orcid.org/0000-0003-2982-3548>
 Simon Scheiter  <https://orcid.org/0000-0002-5449-841X>

REFERENCES

- Ainsworth, E. A., & Rogers, A. (2007). The response of photosynthesis and stomatal conductance to rising [CO₂]: Mechanisms and environmental interactions. *Plant, Cell & Environment*, 30, 258–270. <https://doi.org/10.1111/j.1365-3040.2007.01641.x>
- Allen, R. G., Pereira, L. S., Raes, D., & Smith, M. (1998). *Crop evapotranspiration: Guidelines for computing crop water requirements*. FAO Irrigation and Drainage Paper No. 56, FAO.
- Archer, E., Engelbrecht, F., Hänslar, A., Landman, W., Tadross, M., & Helmschrot, J. (2018). Seasonal prediction and regional climate projections for southern Africa. *Biodiversity & Ecology*, 6, 14–21. <https://doi.org/10.7809/b-e.00296>
- Avitabile, V., Herold, M., Heuvelink, G. B. M., Lewis, S. L., Phillips, O. L., Asner, G. P., Armston, J., Ashton, P. S., Banin, L., Bayol, N., Berry, N. J., Boeckx, P., de Jong, B. H. J., DeVries, B., Girardin, C. A. J., Kearsley, E., Lindsell, J. A., Lopez-Gonzalez, G., Lucas, R., ... Willcock, S. (2016). An integrated pan-tropical biomass map using multiple reference datasets. *Global Change Biology*, 22, 1406–1420. <https://doi.org/10.1111/gcb.13139>
- Baccini, A., Goetz, S. J., Walker, W. S., Laporte, N. T., Sun, M., Sulla-Menashe, D., Hackler, J., Beck, P. S. A., Dubayah, R., Friedl, M. A., Samanta, S., & Houghton, R. A. (2012). Estimated carbon dioxide emissions from tropical deforestation improved by carbon-density maps. *Nature Climate Change*, 2, 182–185. <https://doi.org/10.1038/nclimate1354>
- Ball, J. T., Woodrow, I. E., & Berry, J. A. (1987). A model predicting stomatal conductance and its contribution to the control of photosynthesis under different environmental conditions. In J. Biggins (Ed.), *Progress in photosynthesis research* (pp. 221–224). Martinus-Nijhoff Publishers.
- Bombelli, A., Henry, M., Castaldi, S., Adu-Bredu, S., Arneith, A., de Grandcourt, A., Grieco, E., Kutsch, W. L., Lehsten, V., Rasile, A., Reichstein, M., Tansley, K., Weber, U., & Valentini, R. (2009). An outlook on the Sub-Saharan Africa carbon balance. *Biogeosciences*, 6, 2193–2205. <https://doi.org/10.5194/bg-6-2193-2009>
- Bond, W. J. (2016). Ancient grasslands at risk. *Science*, 351, 120–122. <https://doi.org/10.1126/science.aad5132>
- Bond, W. J., & Midgley, G. F. (2000). A proposed CO₂-controlled mechanism of woody plant invasion in grasslands and savannas. *Global Change Biology*, 6, 865–869. <https://doi.org/10.1046/j.1365-2486.2000.00365.x>
- Bond, W. J., & Midgley, G. F. (2012). Carbon dioxide and the uneasy interactions of trees and savannah grasses. *Philosophical Transactions of the Royal Society B*, 367, 601–612. <https://doi.org/10.1098/rstb.2011.0182>
- Bond, W. J., & Midgley, J. J. (2001). Ecology of sprouting in woody plants: The persistence niche. *Trends in Ecology & Evolution*, 16, 45–51. [https://doi.org/10.1016/S0169-5347\(00\)02033-4](https://doi.org/10.1016/S0169-5347(00)02033-4)
- Bond, W. J., Stevens, N., Midgley, G. F., & Lehmann, C. E. (2019). The trouble with trees: Afforestation plans for Africa. *Trends in Ecology & Evolution*, 34(11), 963–965. <https://doi.org/10.1016/j.tree.2019.08.003>
- Brancalion, P. H. S., Niamir, A., Broadbent, E., Crouzeilles, R., Barros, F. S. M., Almeyda Zambrano, A. M., Baccini, A., Aronson, J., Goetz, S., Reid, J. L., Strassburg, B. B. N., Wilson, S., & Chazdon, R. L. (2019). Global restoration opportunities in tropical rainforest landscapes. *Science Advances*, 5. <https://doi.org/10.1126/sciadv.aav3223>
- Chapin, F., Matson, P., & Mooney, H. (2011). *Principles of terrestrial ecosystem ecology* (2nd ed.). Springer.
- Collatz, G. J., Ball, J. T., Grivet, C., & Berry, J. A. (1991). Physiological and environmental regulation of stomatal conductance, photosynthesis and transpiration: A model that includes a laminar boundary layer. *Agricultural and Forest Meteorology*, 54, 107–136. [https://doi.org/10.1016/0168-1923\(91\)90002-8](https://doi.org/10.1016/0168-1923(91)90002-8)
- Collatz, G. J., Ribas-Carbo, M., & Berry, J. A. (1992). Coupled photosynthesis-stomatal conductance model for leaves of C₄ plants. *Australian*

- Journal of Plant Physiology*, 19, 519–538. <https://doi.org/10.1071/PP9920519>
- Conradi, T., Slingsby, J. A., Midgley, G. F., Nottebrock, H., Schweiger, A. H., & Higgins, S. I. (2020). An operational definition of the biome for global change research. *New Phytologist*, 227, 1294–1306. <https://doi.org/10.1111/nph.16580>
- Cramer, W., Bondeau, A., Woodward, F. I., Prentice, C., Betts, R. A., Brovkin, V., Cox, P. M., Fisher, V., Foley, J. A., Friend, A. D., Kucharik, C., Lomas, M. R., Ramankutty, N., Sitch, S., Smith, B., White, A., & Young-Molling, C. (2001). Global response of terrestrial ecosystem structure and function to CO₂ and climate change: Results from six dynamic global vegetation models. *Global Change Biology*, 7, 357–373. <https://doi.org/10.1046/j.1365-2486.2001.00383.x>
- Davis-Reddy, C., Vincent, K., & Mambo, J. (2017). Socio-economic impacts of extreme weather events in Southern Africa. In C. Davis-Reddy & K. Vincent (Eds.), *Climate risk and vulnerability: A handbook for Southern Africa* (2nd ed., pp. 30–46). CSIR. Retrieved from https://www.csir.co.za/sites/default/files/Documents/SADC%20Handbook_Second%20Edition_full%20report.pdf
- De Kauwe, M. G., Medlyn, B. E., Zaehle, S., Walker, A. P., Dietze, M. C., Hickler, T., Jain, A. K., Luo, Y., Parton, W. J., Colin Prentice, I., Smith, B., Thornton, P. E., Wang, S., Wang, Y.-P., Wårlind, D., Weng, E., Crous, K. Y., Ellsworth, D. S., Hanson, P. J., ... Norby, R. J. (2013). Forest water use and water use efficiency at elevated CO₂: A model-data intercomparison at two contrasting temperate forest FACE sites. *Global Change Biology*, 19, 1759–1779. <https://doi.org/10.1111/gcb.12164>
- Dietzen, C. A., Larsen, K. S., Ambus, P. L., Michelsen, A., Arndal, M. F., Beier, C., Reinsch, S., & Schmidt, I. K. (2019). Accumulation of soil carbon under elevated CO₂ unaffected by warming and drought. *Global Change Biology*, 25, 9, 2970–2977. <https://doi.org/10.1111/gcb.14699>
- Doherty, R. M., Sitch, S., Smith, B., Lewis, S. L., & Thornton, P. K. (2010). Implications of future climate and atmospheric CO₂ content for regional biogeochemistry, biogeography and ecosystem services across east Africa. *Global Change Biology*, 16, 617–640. <https://doi.org/10.1111/j.1365-2486.2009.01997.x>
- Dufresne, J.-L., Fairhead, L., Le Treut, H., Berthelot, M., Bopp, L., Ciais, P., Friedlingstein, P., & Monfray, P. (2002). On the magnitude of positive feedback between future climate change and the carbon cycle. *Geophysical Research Letters*, 29, 43–1–43–4. <https://doi.org/10.1029/2001GL013777>
- Engelbrecht, C. J., & Engelbrecht, F. A. (2016). Shifts in Köppen-Geiger climate zones over southern Africa in relation to key global temperature goals. *Theoretical and Applied Climatology*, 123, 247–261. <https://doi.org/10.1007/s00704-014-1354-1>
- Engelbrecht, C. J., Engelbrecht, F. A., & Dyson, L. L. (2013). High-resolution model-projected changes in mid-tropospheric closed-lows and extreme rainfall events over southern Africa. *International Journal of Climatology*, 33, 173–187. <https://doi.org/10.1002/joc.3420>
- Engelbrecht, F., Adegoke, J., Bopape, M.-J., Naidoo, M., Garland, R., Thatcher, M., McGregor, J., Katzfey, J., Werner, M., Ichoku, C., & Gatebe, C. (2015). Projections of rapidly rising surface temperatures over Africa under low mitigation. *Environmental Research Letters*, 10, 085004. <https://doi.org/10.1088/1748-9326/10/8/085004>
- Engelbrecht, F. A., McGregor, J. L., & Engelbrecht, C. J. (2009). Dynamics of the conforal cubic atmospheric model projected climate-change signal over southern Africa. *International Journal of Climatology*, 29, 1013–1033. <https://doi.org/10.1002/joc.1742>
- Farquhar, G. D., Caemmerer, S. V., & Berry, J. A. (1980). A biochemical-model of photosynthetic CO₂ assimilation in leaves of C₃ species. *Planta*, 149, 78–90. <https://doi.org/10.1007/BF00386231>
- Fisher, R. A., Koven, C. D., Anderegg, W. R. L., Christoffersen, B. O., Dietze, M. C., Farrior, C. E., Holm, J. A., Hurtt, G. C., Knox, R. G., Lawrence, P. J., Lichstein, J. W., Longo, M., Matheny, A. M., Medvigy, D., Muller-Landau, H. C., Powell, T. L., Serbin, S. P., Sato, H., Shuman, J. K., ... Moorcroft, P. R. (2018). Vegetation demographics in Earth System Models: A review of progress and priorities. *Global Change Biology*, 24, 35–54. <https://doi.org/10.1111/gcb.13910>
- Fleischer, K., Rammig, A., De Kauwe, M. G., Walker, A. P., Domingues, T. F., Fuchsluger, L., Garcia, S., Goll, D. S., Grandis, A., Jiang, M., Haverd, V., Hofhansl, F., Holm, J. A., Kruijt, B., Leung, F., Medlyn, B. E., Mercado, L. M., Norby, R. J., Pak, B., ... Lapola, D. M. (2019). Amazon forest response to CO₂ fertilization dependent on plant phosphorus acquisition. *Nature Geoscience*, 12, 736–741. <https://doi.org/10.1038/s41561-019-0404-9>
- Fletcher, S., Lickley, M., & Strzepek, K. (2019). Learning about climate change uncertainty enables flexible water infrastructure planning. *Nature Communications*, 10, 1782. <https://doi.org/10.1038/s41467-019-09677-x>
- Global Soil Data Task Group. (2000). Global gridded surfaces of selected soil characteristics (igbp-dis). <https://doi.org/10.3334/ORNLD AAC/569>
- Gonzalez, P., Neilson, R. P., Lenihan, J. M., & Drapek, R. J. (2010). Global patterns in the vulnerability of ecosystems to vegetation shifts due to climate change. *Global Ecology and Biogeography*, 19, 755–768. <https://doi.org/10.1111/j.1466-8238.2010.00558.x>
- Gonzalez, P., Tucker, C., & Sy, H. (2012). Tree density and species decline in the African Sahel attributable to climate. *Journal of Arid Environments*, 78, 55–64. <https://doi.org/10.1016/j.jaridenv.2011.11.001>
- Haverd, V., Smith, B., Nieradzki, L., Briggs, P. R., Woodgate, W., Trudinger, C. M., Canadell, J. G., & Cuntz, M. (2018). A new version of the CABLE land surface model (Subversion revision r4601) incorporating land use and land cover change, woody vegetation demography, and a novel optimisation-based approach to plant coordination of photosynthesis. *Geoscientific Model Development*, 11, 2995–3026. <https://doi.org/10.5194/gmd-11-2995-2018>
- Hickler, T., Rammig, A., & Werner, C. (2015). Modelling CO₂ impacts on forest productivity. *Current Forestry Reports*, 1, 69–80. <https://doi.org/10.1007/s40725-015-0014-8>
- Higgins, S. I., Bond, W. J., & Trollope, W. S. W. (2000). Fire, resprouting and variability: A recipe for grass-tree coexistence in savanna. *Journal of Ecology*, 88, 213–229. <https://doi.org/10.1046/j.1365-2745.2000.00435.x>
- Higgins, S. I., Bond, W. J., Trollope, W. S. W., & Williams, R. J. (2008). Physically motivated empirical models for the spread and intensity of grass fires. *International Journal of Wildland Fire*, 17, 595–601. <https://doi.org/10.1071/WF06037>
- Higgins, S. I., Keretsetse, M., & February, E. C. (2015). Feedback of trees on nitrogen mineralization to restrict the advance of trees in C4 savannas. *Biology Letters*, 11, <https://doi.org/10.1098/rsbl.2015.0572>
- Higgins, S. I., & Scheiter, S. (2012). Atmospheric CO₂ forces abrupt vegetation shifts locally, but not globally. *Nature*, 488, 209–212. <https://doi.org/10.1038/nature11238>
- Hoegh-Guldberg, O., Jacob, D., Taylor, M., Bindi, M., Brown, S., Camilloni, I., Diedhiou, A., Djalante, R., Ebi, K. L., Engelbrecht, F., Guiot, J., Hijikata, Y., Mehrotra, S., Payne, A., Seneviratne, S. I., Thomas, A., Warren, R., & Zhou, G. (2018). Impacts of 1.5°C global warming on natural and human systems. In V. Masson-Delmotte, P. Zhai, H.-O. Pörtner, D. Roberts, J. Skea, P. R. Shukla, A. Pirani, W. Moufouma-Okia, C. Péan, R. Pidcock, S. Connors, J. B. R. Matthews, Y. Chen, X. Zhou, M. I. Gomis, E. Lonnoy, T. Maycock, M. Tignor, & T. Waterfield (Eds.), *Global Warming of 1.5°C. An IPCC Special Report on the impacts of global warming of 1.5°C above pre-industrial levels and related global greenhouse gas emission pathways, in the context of strengthening the global response to the threat of climate change, sustainable development, and efforts to eradicate poverty* (pp. 175–311). World Meteorological Organization.
- Hoffmann, W. A., Geiger, E. L., Gotsch, S. G., Rossatto, D. R., Silva, L. C. R., Lau, O. L., Haridasan, M., & Franco, A. C. (2012). Ecological thresholds

- at the savanna-forest boundary: How plant traits, resources and fire govern the distribution of tropical biomes. *Ecology Letters*, 15, 759–768. <https://doi.org/10.1111/j.1461-0248.2012.01789.x>
- Hubau, W., Lewis, S. L., Phillips, O. L., Affum-Baffoe, K., Beeckman, H., Cuni-Sanchez, A., Daniels, A. K., Ewango, C. E. N., Fauset, S., Mukinzi, J. M., Sheil, D., Sonké, B., Sullivan, M. J. P., Sunderland, T. C. H., Taedoumg, H., Thomas, S. C., White, L. J. T., Abernethy, K. A., Adu-Bredu, S., ... Zemagho, L. (2020). Asynchronous carbon sink saturation in African and Amazonian tropical forests. *Nature*, 579, 80–87. <https://doi.org/10.1038/s41586-020-2035-0>
- Huntingford, C., Zelazowski, P., Galbraith, D., Mercado, L. M., Sitch, S., Fisher, R., Lomas, M., Walker, A. P., Jones, C. D., Booth, B. B. B., Malhi, Y., Hemming, D., Kay, G., Good, P., Lewis, S. L., Phillips, O. L., Atkin, O. K., Lloyd, J., Gloor, E., ... Cox, P. M. (2013). Simulated resilience of tropical rainforests to CO₂-induced climate change. *Nature Geoscience*, 6, 268–273. <https://doi.org/10.1038/ngeo1741>
- ILO, International Labour Organization. (2019). *Agriculture as % of total employment – ILO modelled estimates, November 2018*. Department of Statistics, International Labour Organization. <https://www.ilo.org/shinyapps/bulkexplorer6/>
- Jetz, W., & Fine, P. V. A. (2012). Global gradients in vertebrate diversity predicted by historical area-productivity dynamics and contemporary environment. *PLOS Biology*, 10, 1–11. <https://doi.org/10.1371/journal.pbio.1001292>
- Jiang, M., Caldaru, S., Zhang, H., Fleischer, K., Crous, K. Y., Yang, J., De Kauwe, M. G., Ellsworth, D. S., Reich, P. B., Tissue, D. T., & Zaehle, S. (2020). Low phosphorus supply constrains plant responses to elevated CO₂: A meta-analysis. *Global Change Biology*, 26(10), 5856–5873. <https://doi.org/10.1111/gcb.15277>
- Jiang, M., Medlyn, B. E., Drake, J. E., Duursma, R. A., Anderson, I. C., Barton, C. V. M., Boer, M. M., Carrillo, Y., Castañeda-Gómez, L., Collins, L., Crous, K. Y., De Kauwe, M. G., dos Santos, B. M., Emmerson, K. M., Facey, S. L., Gherlenda, A. N., Gimeno, T. E., Hasegawa, S., Johnson, S. N., ... Ellsworth, D. S. (2020). The fate of carbon in a mature forest under carbon dioxide enrichment. *Nature*, 580, 227–323. <https://doi.org/10.1038/s41586-020-2128-9>
- Kgope, B. S., Bond, W. J., & Midgley, G. F. (2010). Growth responses of African savanna trees implicate atmospheric [CO₂] as a driver of past and current changes in savanna tree cover. *Austral Ecology*, 35, 451–463. <https://doi.org/10.1111/j.1442-9993.2009.02046.x>
- Körner, C. (2015). Paradigm shift in plant growth control. *Current Opinion in Plant Biology*, 25, 107–114. <https://doi.org/10.1016/j.pbi.2015.05.003>
- Körner, C., Asshoff, R., Bignucolo, O., Hättenschwiler, S., Keel, S. G., Peláez-Riedl, S., Pepin, S., Siegwolf, R. T. W., & Zotz, G. (2005). Carbon flux and growth in mature deciduous forest trees exposed to elevated CO₂. *Science*, 309, 1360–1362. <https://doi.org/10.1126/science.1113977>
- Liu, Y., van Dijk, A. I. J. M., de Jeu, R. A. M., Canadell, J. G., McCabe, M. F., Evans, J. P., & Wang, G. (2015). Recent reversal in loss of global terrestrial biomass. *Nature Climate Change*, 5, 470–474. <https://doi.org/10.1038/nclimate2581>
- Loidi, J., & Fernández-González, F. (2012). Potential natural vegetation: Reburying or reboring? *Journal of Vegetation Science*, 23, 596–604. <https://doi.org/10.1111/j.1654-1103.2012.01387.x>
- Long, S. P., Ainsworth, E. A., Rogers, A., & Ort, D. R. (2004). Rising atmospheric carbon dioxide: Plants face the future. *Annual Review of Plant Biology*, 55, 591–628. <https://doi.org/10.1146/annurev.arpla.55.031903.141610>
- McGregor, J. L. (2005). C-CAM: Geometric aspects and dynamical formulation. <http://www.cmar.csiro.au/e-print/open/mcgregor2005a.pdf>
- Medlyn, B. E., Barton, C. V. M., Broadmeadow, M. S. J., Ceulemans, R., De Angelis, P., Forstreuter, M., Freeman, M., Jackson, S. B., Kellomäki, S., Laitat, E., Rey, A., Roberntz, P., Sigurdsson, B. D., Strassmeyer, J., Wang, K., Curtis, P. S., & Jarvis, P. G. (2001). Stomatal conductance of forest species after long-term exposure to elevated CO₂ concentration: A synthesis. *New Phytologist*, 149, 247–264. <https://doi.org/10.1046/j.1469-8137.2001.00028.x>
- Medlyn, B. E., Zaehle, S., De Kauwe, M. G., Walker, A. P., Dietze, M. C., Hanson, P. J., Hickler, T., Jain, A. K., Luo, Y., Parton, W., Prentice, I. C., Thornton, P. E., Wang, S., Wang, Y.-P., Weng, E., Iversen, C. M., McCarthy, H. R., Warren, J. M., Oren, R., & Norby, R. J. (2015). Using ecosystem experiments to improve vegetation models. *Nature Climate Change*, 5, 528–534. <https://doi.org/10.1038/NCLIMATE2621>
- Midgley, G. F., & Bond, W. J. (2015). Future of African terrestrial biodiversity and ecosystems under anthropogenic climate change. *Nature Climate Change*, 5, 823–829. <https://doi.org/10.1038/nclimate2753>
- Moncrieff, G. R., Scheiter, S., Bond, W. J., & Higgins, S. I. (2014). Increasing atmospheric CO₂ overrides the historical legacy of multiple stable biome states in Africa. *New Phytologist*, 201, 908–915. <https://doi.org/10.1111/nph.12551>
- Morales, P., Hickler, T., Rowell, D. P., Smith, B., & Sykes, M. T. (2007). Changes in European ecosystem productivity and carbon balance driven by regional climate model output. *Global Change Biology*, 13, 108–122. <https://doi.org/10.1111/j.1365-2486.2006.01289.x>
- Müller, C., Waha, K., Bondeau, A., & Heinke, J. (2014). Hotspots of climate change impacts in Sub-Saharan Africa and implications for adaptation and development. *Global Change Biology*, 20, 2505–2517. <https://doi.org/10.1111/gcb.12586>
- Naidoo, R., Balmford, A., Costanza, R., Fisher, B., Green, R. E., Lehner, B., Malcolm, T. R., & Ricketts, T. H. (2008). Global mapping of ecosystem services and conservation priorities. *Proceedings of the National Academy of Sciences of the United States of America*, 105, 9495–9500. <https://doi.org/10.1073/pnas.0707823105>
- New, M., Lister, D., Hulme, M., & Makin, I. (2002). A high-resolution data set of surface climate over global land areas. *Climate Research*, 21, 1–25. <https://doi.org/10.3354/cr021001>
- Niang, I., Ruppel, O., Abdrabo, M., Essel, A., Lennard, C., Padgham, J., & Urquhart, P. (2014). *Climate change 2014: Impacts, adaptation, and vulnerability. Part B: Regional aspects. Contribution of working group II to the fifth assessment report of the Intergovernmental Panel on Climate Change, chap. Africa* (pp. 1199–1265). Cambridge University Press.
- Nishina, K., Ito, A., Falloon, P., Friend, A. D., Beerling, D. J., Ciais, P., Clark, D. B., Kahana, R., Kato, E., Lucht, W., Lomas, M., Pavlick, R., Schaphoff, S., Warszawski, L., & Yokohata, T. (2015). Decomposing uncertainties in the future terrestrial carbon budget associated with emission scenarios, climate projections, and ecosystem simulations using the ISI-MIP results. *Earth System Dynamics*, 6, 435–445. <https://doi.org/10.5194/esd-6-435-2015>
- Norby, R. J., De Kauwe, M. G., Domingues, T. F., Duursma, R. A., Ellsworth, D. S., Goll, D. S., Lapola, D. M., Luus, K. A., Rob MacKenzie, A., Medlyn, B. E., Pavlick, R., Rammig, A., Smith, B., Thomas, R., Thonicke, K., Walker, A. P., Yang, X., & Zaehle, S. (2016). Model-data synthesis for the next generation of forest free-air CO₂ enrichment (FACE) experiments. *New Phytologist*, 209, 17–28. <https://doi.org/10.1111/nph.13593>
- Norby, R. J., Warren, J. M., Iversen, C. M., Medlyn, B. E., & McMurtrie, R. E. (2010). CO₂ enhancement of forest productivity constrained by limited nitrogen availability. *Proceedings of the National Academy of Sciences of the United States of America*, 107, 19368–19373. <https://doi.org/10.1073/pnas.1006463107>
- Nowak, R. S., Ellsworth, D. S., & Smith, S. D. (2004). Functional responses of plants to elevated atmospheric CO₂ – Do photosynthetic and productivity data from FACE experiments support early predictions? *New Phytologist*, 162(2), 253–280. <https://doi.org/10.1111/j.1469-8137.2004.01033.x>
- O'Connor, T. G., Puttick, J. R., & Hoffman, M. T. (2014). Bush encroachment in southern Africa: Changes and causes. *African Journal of*

- Range & Forage Science*, 31, 67–88. <https://doi.org/10.2989/10220119.2014.939996>
- Olejnik, S., & Algina, J. (2003). Generalized eta and omega squared statistics: Measures of effect size for some common research designs. *Psychological Methods*, *American Psychological Association*, 8, 434–447. <https://doi.org/10.1037/1082-989X.8.4.434>
- Osborne, C. P., Charles-Dominique, T., Stevens, N., Bond, W. J., Midgley, G., & Lehmann, C. E. R. (2018). Human impacts in African savannas are mediated by plant functional traits. *New Phytologist*, *220*(1), 10–24. <https://doi.org/10.1111/nph.15236>
- Parr, C. L., Lehmann, C. E., Bond, W. J., Hoffmann, W. A., & Andersen, A. N. (2014). Tropical grassy biomes: Misunderstood, neglected, and under threat. *Trends in Ecology & Evolution*, *29*, 205–213. <https://doi.org/10.1016/j.tree.2014.02.004>
- Peñuelas, J., Canadell, J. G., & Ogaya, R. (2011). Increased water-use efficiency during the 20th century did not translate into enhanced tree growth. *Global Ecology and Biogeography*, *20*, 597–608. <https://doi.org/10.1111/j.1466-8238.2010.00608.x>
- Pfeiffer, M., Langan, L., Linstädter, A., Martens, C., Gaillard, C., Ruppert, J. C., Higgins, S. I., Mudongo, E. I., & Scheiter, S. (2019). Grazing and aridity reduce perennial grass abundance in semi-arid rangelands – Insights from a trait-based dynamic vegetation model. *Ecological Modelling*, *395*, 11–22. <https://doi.org/10.1016/j.ecolmodel.2018.12.013>
- Popp, A., Calvin, K., Fujimori, S., Havlik, P., Humpenöder, F., Stehfest, E., Bodirsky, B. L., Dietrich, J. P., Doelmann, J. C., Gusti, M., Hasegawa, T., Kyle, P., Obersteiner, M., Tabeau, A., Takahashi, K., Valin, H., Waldhoff, S., Weindl, I., Wise, M., ... Vuuren, D. P. V. (2017). Land-use futures in the shared socio-economic pathways. *Global Environmental Change*, *42*, 331–345. <https://doi.org/10.1016/j.gloenvcha.2016.10.002>
- Prentice, I. C., Bondeau, A., Cramer, W., Harrison, S. P., Hickler, T., Lucht, W., Sitch, S., Smith, B., & Sykes, M. T. (2007). Dynamic global vegetation modeling: Quantifying terrestrial ecosystem responses to large-scale environmental change (pp. 175–192). Springer. https://doi.org/10.1007/978-3-540-32730-1_15
- R Core Team. (2015). *R: A language and environment for statistical computing*. R Foundation for Statistical Computing. <https://www.R-project.org/>
- Rammig, A., Jupp, T., Thonicke, K., Tietjen, B., Heinke, J., Ostberg, S., Lucht, W., Cramer, W., & Cox, P. (2010). Estimating the risk of Amazonian forest dieback. *New Phytologist*, *187*, 694–706. <https://doi.org/10.1111/j.1469-8137.2010.03318.x>
- Ratnam, J., Bond, W. J., Fensham, R. J., Hoffmann, W. A., Archibald, S., Lehmann, C. E. R., Anderson, M. T., Higgins, S. I., & Sankaran, M. (2011). When is a 'forest' a savanna, and why does it matter? *Global Ecology and Biogeography*, *20*, 653–660. <https://doi.org/10.1111/j.1466-8238.2010.00634.x>
- Reich, P. B., Hobbie, S. E., & Lee, T. D. (2014). Plant growth enhancement by elevated CO₂ eliminated by joint water and nitrogen limitation. *Nature Geoscience*, *7*, 920–924. <https://doi.org/10.1038/ngeo2284>
- Saatchi, S. S., Harris, N. L., Brown, S., Lefsky, M., Mitchard, E. T. A., Salas, W., Zutta, B. R., Buermann, W., Lewis, S. L., Hagen, S., Petrova, S., White, L., Silman, M., & Morel, A. (2011). Benchmark map of forest carbon stocks in tropical regions across three continents. *Proceedings of the National Academy of Sciences of the United States of America*, *108*, 9899–9904. <https://doi.org/10.1073/pnas.1019576108>
- Sato, H., & Ise, T. (2012). Effect of plant dynamic processes on African vegetation responses to climate change: Analysis using the spatially explicit individual-based dynamic global vegetation model (SEIB-DGVM). *Journal of Geophysical Research: Biogeosciences*, *117*, G03017. <https://doi.org/10.1029/2012JG002056>
- Scheiter, S., Gaillard, C., Martens, C., Erasmus, B., & Pfeiffer, M. (2018). How vulnerable are ecosystems in the Limpopo province to climate change? *South African Journal of Botany*, *116*, 86–95. <https://doi.org/10.1016/j.sajb.2018.02.394>
- Scheiter, S., & Higgins, S. I. (2009). Impacts of climate change on the vegetation of Africa: An adaptive dynamic vegetation modeling approach. *Global Change Biology*, *15*, 2224–2246. <https://doi.org/10.1111/j.1365-2486.2008.01838.x>
- Scheiter, S., Higgins, S. I., Beringer, J., & Hutley, L. B. (2015). Climate change and long-term fire management impacts on Australian savannas. *New Phytologist*, *205*, 1211–1226. <https://doi.org/10.1111/nph.13130>
- Scheiter, S., Higgins, S. I., Osborne, C. P., Bradshaw, C., Lunt, D., Ripley, B. S., Taylor, L. L., & Beerling, D. J. (2012). Fire and fire-adapted vegetation promoted C₄ expansion in the late Miocene. *New Phytologist*, *195*, 653–666. <https://doi.org/10.1111/j.1469-8137.2012.04202.x>
- Scheiter, S., Kumar, D., Corlett, R. T., Gaillard, C., Langan, L., Lapuz, R. S., Martens, C., Pfeiffer, M., & Tomlinson, K. W. (2020). Climate change promotes transitions to tall evergreen vegetation in tropical Asia. *Global Change Biology*, *26*(9), 5106–5124. <https://doi.org/10.1111/gcb.15217>
- Scheiter, S., & Savadogo, P. (2016). Ecosystem management can mitigate vegetation shifts induced by climate change in West Africa. *Ecological Modelling*, *332*, 19–27. <https://doi.org/10.1016/j.ecolmodel.2016.03.022>
- Scheiter, S., Schulte, J., Pfeiffer, M., Martens, C., Erasmus, B. F., & Twine, W. C. (2019). How does climate change influence the economic value of ecosystem services in savanna rangelands? *Ecological Economics*, *157*, 342–356. <https://doi.org/10.1016/j.ecolecon.2018.11.015>
- Scholze, M., Knorr, W., Arnell, N. W., & Prentice, I. C. (2006). A climate-change risk analysis for world ecosystems. *Proceedings of the National Academy of Sciences of the United States of America*, *103*, 13116–13120. <https://doi.org/10.1073/pnas.0601816103>
- Shi, M., Fisher, J. B., Brzostek, E. R., & Phillips, R. P. (2016). Carbon cost of plant nitrogen acquisition: Global carbon cycle impact from an improved plant nitrogen cycle in the Community Land Model. *Global Change Biology*, *22*, 1299–1314. <https://doi.org/10.1111/gcb.13131>
- Silva, L. C. R., & Anand, M. (2013). Probing for the influence of atmospheric CO₂ and climate change on forest ecosystems across biomes. *Global Ecology and Biogeography*, *22*, 83–92. <https://doi.org/10.1111/j.1466-8238.2012.00783.x>
- Sitch, S., Huntingford, C., Gedney, N., Levy, P. E., Lomas, M., Piao, S. L., Betts, R., Ciais, P., Cox, P., Friedlingstein, P., Jones, C. D., Prentice, I. C., & Woodward, F. I. (2008). Evaluation of the terrestrial carbon cycle, future plant geography and climate-carbon cycle feedbacks using five dynamic global vegetation models (DGVMs). *Global Change Biology*, *14*, 2015–2039. <https://doi.org/10.1111/j.1365-2486.2008.01626.x>
- Staver, A. C., Archibald, S., & Levin, S. A. (2011). The global extent and determinants of savanna and forest as alternative biome states. *Science*, *334*, 230–232. <https://doi.org/10.1126/science.1210465>
- Stevens, N., Lehmann, C. E. R., Murphy, B. P., & Durigan, G. (2017). Savanna woody encroachment is widespread across three continents. *Global Change Biology*, *23*, 235–244. <https://doi.org/10.1111/gcb.13409>
- Stocker, T. F., Qin, D., Plattner, G.-K., Alexander, L. V., Allen, S. K., Bindoff, N. L., Bréon, F.-M., Church, J. A., Cubasch, U., Emori, S., Forster, P., Friedlingstein, P., Gillett, N., Gregory, J. M., Hartmann, D. L., Jansen, E., Kirtman, B., Knutti, R., Krishna Kumar, K., ... Xie, S.-P. (2013). Technical summary. In T. F. Stocker, D. Qin, G.-K. Plattner, M. Tignor, S. K. Allen, J. Boschung, A. Nauels, Y. Xia, V. Bex, & P. M. Midgley (Eds.), *Climate change 2013: The physical science basis. Contribution of working group I to the fifth assessment report of the intergovernmental panel on climate change* (pp. 33–115). Cambridge University Press.
- Stokes, C., Ash, A., Tibbett, M., & Holtum, J. (2005). Ozface: The Australian savanna free air CO₂ enrichment facility and its relevance

- to carbon-cycling issues in a tropical savanna. *Australian Journal of Botany*, 53, 677–687. <https://doi.org/10.1071/BT04140>
- Taylor, S. H., Ripley, B. S., Woodward, F. I., & Osborne, C. P. (2011). Drought limitation of photosynthesis differs between C₃ and C₄ grass species in a comparative experiment. *Plant, Cell & Environment*, 34, 65–75. <https://doi.org/10.1111/j.1365-3040.2010.02226.x>
- Terrer, C., Jackson, R. B., Prentice, I. C., Keenan, T. F., Kaiser, C., Vicca, S., Fisher, J. B., Reich, P. B., Stocker, B. D., Hungate, B. A., Peñuelas, J., McCallum, I., Soudzilovskaia, N. A., Cernusak, L. A., Talhelm, A. F., Van Sundert, K., Piao, S., Newton, P. C. D., Hovenden, M. J., ... Franklin, O. (2019). Nitrogen and phosphorus constrain the CO₂ fertilization of global plant biomass. *Nature Climate Change*, 9(9), 684–689. <https://doi.org/10.1038/s41558-019-0545-2>
- Terrer, C., Vicca, S., Hungate, B. A., Phillips, R. P., & Prentice, I. C. (2016). Mycorrhizal association as a primary control of the CO₂ fertilization effect. *Science*, 353, 72–74. <https://doi.org/10.1126/science.aaf4610>
- Terrer, C., Vicca, S., Stocker, B. D., Hungate, B. A., Phillips, R. P., Reich, P. B., Finzi, A. C., & Colin Prentice, I. (2018). Ecosystem responses to elevated CO₂ governed by plant-soil interactions and the cost of nitrogen acquisition. *New Phytologist*, 217, 507–522. <https://doi.org/10.1111/nph.14872>
- van der Slepen, P., Groenendijk, P., Vlam, M., Anten, N. P. R., Boom, A., Bongers, F., Pons, T. L., Terburg, G., & Zuidema, P. A. (2015). No growth stimulation of tropical trees by 150 years of CO₂ fertilization but water-use efficiency increased. *Nature Geoscience*, 8, 24–28. <https://doi.org/10.1038/ngeo2313>
- Veldman, J. W., Overbeck, G. E., Negreiros, D., Mahy, G., Le Stradic, S., Fernandes, G. W., Durigan, G., Buisson, E., Putz, F. E., & Bond, W. J. (2015). Where tree planting and forest expansion are bad for biodiversity and ecosystem services. *BioScience*, 65, 1011–1018. <https://doi.org/10.1093/biosci/biv118>
- Warren, J. M., Pötzelsberger, E., Wullschlegel, S. D., Thornton, P. E., Hasenauer, H., & Norby, R. J. (2011). Ecohydrologic impact of reduced stomatal conductance in forests exposed to elevated CO₂. *Ecohydrology*, 4, 196–210. <https://doi.org/10.1002/eco.173>
- Warszawski, L., Frieler, K., Huber, V., Piontek, F., Serdeczny, O., & Schewe, J. (2014). The inter-sectoral impact model intercomparison project (ISI-MIP): Project framework. *Proceedings of the National Academy of Sciences of the United States of America*, 111, 3228–3232. <https://doi.org/10.1073/pnas.1312330110>
- Weaver, C. P., Lempert, R. J., Brown, C., Hall, J. A., Revell, D., & Sarewitz, D. (2013). Improving the contribution of climate model information to decision making: The value and demands of robust decision frameworks. *Wires: Wiley Interdisciplinary Reviews: Climate Change*, 4, 39–60. <https://doi.org/10.1002/wcc.202>
- White, J. W., Rassweiler, A., Samhouri, J. F., Stier, A. C., & White, C. (2014). Ecologists should not use statistical significance tests to interpret simulation model results. *Oikos*, 123, 385–388. <https://doi.org/10.1111/j.1600-0706.2013.01073.x>
- Yousefpour, R., Jacobsen, J. B., Thorsen, B. J., Meilby, H., Hanewinkel, M., & Oehler, K. (2012). A review of decision-making approaches to handle uncertainty and risk in adaptive forest management under climate change. *Annals of Forest Science*, 69, 1–15. <https://doi.org/10.1007/s13595-011-0153-4>
- Zaehle, S., Medlyn, B. E., De Kauwe, M. G., Walker, A. P., Dietze, M. C., Hickler, T., Luo, Y., Wang, Y.-P., El-Masri, B., Thornton, P., Jain, A., Wang, S., Warlind, D., Weng, E., Parton, W., Iversen, C. M., Gallet-Budynek, A., McCarthy, H., Finzi, A., ... Norby, R. J. (2014). Evaluation of 11 terrestrial carbon-nitrogen cycle models against observations from two temperate Free-Air CO₂ Enrichment studies. *New Phytologist*, 202, 803–822. <https://doi.org/10.1111/nph.12697>

SUPPORTING INFORMATION

Additional supporting information may be found online in the Supporting Information section.

How to cite this article: Martens C, Hickler T, Davis-Reddy C, et al. Large uncertainties in future biome changes in Africa call for flexible climate adaptation strategies. *Glob Change Biol*. 2020;00:1–19. <https://doi.org/10.1111/gcb.15390>